

A critical assessment of satellite drag and atmospheric density modeling[☆]

David A. Vallado*, David Finkleman¹

Center for Space Standards and Innovation, 7150 Campus Dr., Suite 260, Colorado Springs, CO 80920-6522, United States



ARTICLE INFO

Article history:

Received 23 May 2013

Received in revised form

1 October 2013

Accepted 8 October 2013

Available online 25 October 2013

Keywords:

Atmospheric drag

Satellite propagation

Parameters affecting atmospheric drag

Space weather data

Atmospheric density

Space situational awareness

ABSTRACT

This paper examines atmospheric drag models and data usage involved with propagating near-Earth satellites. Many studies, and even some International standards try to promote one model over another, rather than identifying the behavior of the numerous parameters necessary to select the best model for a particular mission and application. We briefly summarize existing information, and quantify sources of uncertainty in satellite propagation resulting from several atmospheric models, or from the treatment of input data indices. The goal is for researchers to understand the relative impact of using different models and data indices so they can properly assess which model and data input to use.

© 2013 IAA. Published by Elsevier Ltd. All rights reserved.

1. Introduction

Significant research has taken place to determine the proper modeling for atmospheric density. The literature contains information in several different disciplines, ranging from basic physics, aerodynamic gas/surface dynamic interactions, orbit determination approaches, to complex models of density, and corrections to existing atmospheric models. Much of the basic research took place almost a half century ago. Jacchia [8], ... began a series of atmospheric models that are still in use today. Gaposchkin and Coster [5] evaluated various atmospheric models and found that none solved all the problems of the day. Today,

we are in a similar situation, but with significantly more models and data to choose from. Nonetheless, the orbit estimation community often overlooks the assumptions upon which atmospheric models were developed, and vice versa.

Atmospheric models generally use parameters based on observables that are considered indicators of atmospheric density, which are often difficult to measure directly (a_p or K_p , and $F_{10.7}$). Researchers often fix one parameter, such as the drag coefficient, and add others to the state vector to be estimated. In some cases, such as spherical objects, this is appropriate. But for more complex shapes this simply moves the uncertainty to another parameter that might not have any real physical connection to the observables. Occasionally, researchers neglect to recognize that the drag coefficients they estimate depend on the model and assumptions they invoke to make the estimates. This leads to physically unrealistic outcomes.

This paper seeks to clarify the sources of uncertainty in the drag problem, both from the literature, and also from experiments we conducted using various atmospheric

* This is a revision to paper AIAA-2008-6442 presented at the AIAA/AAS Astrodynamics Specialist Conference in Honolulu HI, August 17–21, 2008 and at the AGI Users conference, October 2008.

* Corresponding author. Tel.: +1 719 573 2600, direct +610 981 8614; fax: +1 719 573 9079.

E-mail addresses: dvallado@agi.com, davallado@gmail.com.

(D.A. Vallado), finklemand@skysentry.net (D. Finkleman).

¹ Phone +719 573 2600, direct +610 981 8619, fax: +719 573 9079.

models, and by treating the input data differently. Much of the work is inherently related to orbit determination and we use the Kalman filter in Analytical Graphic Inc's Orbit Determination Toolkit (ODTK). This program is used in many operational and high precision applications because it is trusted as a robust, flexible, and highly accurate processing platform. Not all atmospheric models are tested, nor would it be practical to present data from all the models that exist today. We select from ODTK's available models to expose the characteristics one will find when evaluating models for a particular application.

An important overall consideration is stated. We use propagation comparisons to estimate the effect of various configurations throughout the paper. This is insufficient to accurately measuring what an actual satellite would experience over time, as well as the intricate coupling of all forces, but we are simply trying to demonstrate that several common practices may actually insert significant uncertainty into the solution. The prediction interval is also an important consideration. A 4 to 8-day prediction interval shows the dominant effects. Longer spans risk unnecessarily large errors, and shorter spans may not show the overall effect of input choices and operations. Thus, our approach throughout the paper is to isolate (as much as possible) all other factors and variables, and examine only one item at a time to try and obtain its' contribution to the overall accuracy and operation of using atmospheric drag for satellite calculations.

There are five major areas that we examine (see Fig. 1). This is our approach to organizing and examining the coupled issues of atmospheric density and its effect on

satellite motion. In some cases we are able to develop metrics to indicate the effect of one parameter on the overall accuracy. We examine the predominant approaches to predicting atmospheric drag forces. We discuss physical inconsistencies in determining and employing approximations to thermospheric density, and drag coefficients. This should be considered a framework to guide the researcher to an internally consistent approach for calculating atmospheric drag effects on a satellite.

1.1. Basic introduction

There are two fundamental operations that are involved in atmospheric drag: the determination of atmospheric density, and the interaction of the satellite surface with the atmosphere. Much of the recent literature deals with the former, but the latter is an equally important component to the overall effect of atmospheric density on satellite orbits. We examine the case where we have tracking data for satellite objects, determine the ballistic coefficient from the observations, and then use it for predictions.

Ref. [27], Sec 8.6.2 provides the basic fundamentals related to atmospheric drag so we will not repeat all that information here. The widely accepted equation for the acceleration imparted on the satellite from atmospheric drag is

$$\vec{a}_{\text{drag}} = -\frac{1}{2}\rho \frac{c_D A}{m} v_{\text{rel}}^2 \frac{\vec{v}_{\text{rel}}}{|\vec{v}_{\text{rel}}|} \quad (1)$$

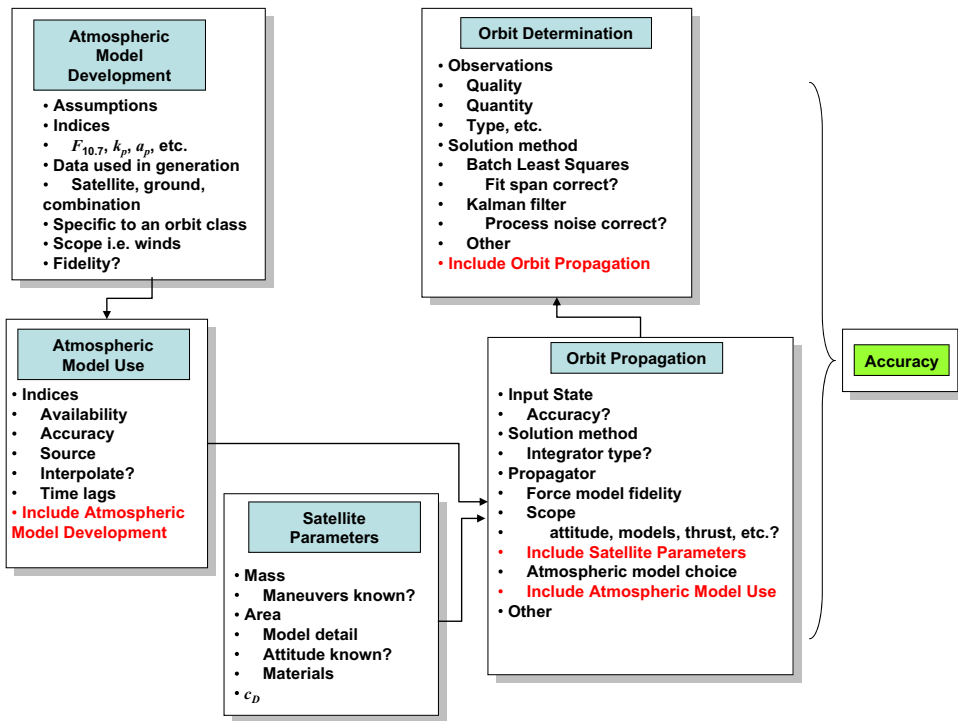


Fig. 1. Variables in the determination of atmospheric drag. Several disciplines are required to properly model atmospheric drag. The relationships show the broad areas we will explore. Note that each of these areas have error bars, some of which are significant. None of them are without error, and many are inter-related.

Here m is the satellite mass, A is the satellite area, \vec{v}_{rel} is the relative velocity, or the satellite velocity relative to the rotating atmosphere, and c_D is the coefficient of drag. Despite the innocuous form, atmospheric drag is probably the most elusive of the force models used for satellite operations because in reality, *all* of the parameters vary over time.

Atmospheric drag forces are the consequence of a satellite doing work on the atmosphere. Momentum and energy are exchanged between the satellite and the atmosphere. The nature of the momentum exchange depends on the distribution of mass in the atmosphere and the geometry and characteristics of the surface of the satellite. The duration of the encounter between an element of the atmosphere and the satellite is important. A simple approximation of c_D

$$c_D = \frac{2m|\vec{a}_{drag}|}{\rho v_{rel}^2 A} \quad (2)$$

is valid only when the length scale of the problem is much greater than the mean free path between collisions among gas particles or the duration of the interaction between the atmosphere and the satellite is much greater than the time between particle collisions. There has to be enough time for collisions among gas particles to equilibrate the consequences of the interaction. The dependence of drag force upon area, velocity, and density is not necessarily as straightforward in the sparse atmosphere of orbital regimes. The drag coefficient compares inertial forces to the dynamic pressure acting on the area presented to the flow. The density, velocity, and area are variables of the problem. They normalize forces so that c_D is non-dimensional. As long as density and velocity do not vary much along the orbit, this is sufficient. If drag scales with dynamic pressure, c_D should be a constant for a given orientation of the satellite. The equations of motion can be integrated as though drag force depends on instantaneous local velocity squared and with a density that varies along the flight path. This scaling does not necessarily hold in unsteady, nonequilibrium situations.

This approximation is valid for hypervelocity, continuum flow. If the oncoming flow is reflected from a vertical surface, the drag is twice the momentum of the free stream intercepted by the surface, $c_D=4$. If the surface were inclined at 45 degrees and the oncoming flow deflected upward, $c_D=2$, and there would be a corresponding downward force on the surface. ***This roughly bounds drag coefficient***, but it is not sufficient for accurate prediction of the drag force. Using Eq. (6), we estimate the significance of drag relative to other forces that a satellite experiences Fig. 2.

The relative velocity depends on the accuracy of the *a priori* estimate, and the results of any orbit determination processes. Because it's generally large, and squared, it becomes a very important factor in the calculation of the acceleration, yet it has received surprisingly little analysis in the literature. A common assumption is that the lower atmosphere rotates with the Earth, allowing a vector summation for the velocity values. The upper atmosphere winds can be several hundred m/s [5] which can have a

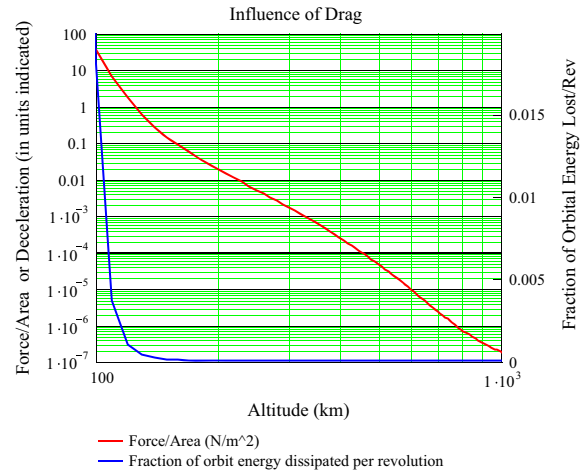


Fig. 2. Influence of Drag for a 1000 kg satellite, 100 m² drag area, and $c_D=2.2$. Harris-Preister model atmosphere.

large effect of the drag acceleration. However, they are particularly unknown, un-modeled, and unpredicted.

$$\vec{v}_{rel} = \vec{v}_{sat} + \vec{v}_{atmos}. \quad (3)$$

The other parameter we do not mention specifically in the following sections is the actual density. Density is a product of all the other parameters we discuss, but ultimately, it's the atmospheric density that affects the trajectory of the satellite. The density usually depends on the atmospheric model, EUV, $F_{10.7}$, K_p , a_p , prediction capability, atmospheric composition, etc. There are a lot of parameters here, each can cause significant changes, and each has uncertainty both in measured values and in prediction. The popular parameters to examine today are the density and the exospheric temperatures. This single parameter represents the largest contribution to error in any orbit determination application.

2. Atmospheric model development

Developing atmospheric models is extremely difficult and time consuming, but there are a plethora of available models. Fewer new models have appeared in recent years with the largest advances coming in the form of corrections to existing models. Because of data availability problems and other technological limitations, many of the early models were focused more on the theoretical implications that could be modeled. For instance, the early Jacchia model (J60 for instance) was more a “mean” approach as compared to the modern NRLMSISE-00 which is an atmospheric constituent based model that tries to accurately model molecular compositions at different altitudes, and hence the overall density. Fig. 3 shows some of the models ([27]:566).

2.1. Assumptions

There are numerous assumptions that are required when creating an atmospheric model. In fact, there are

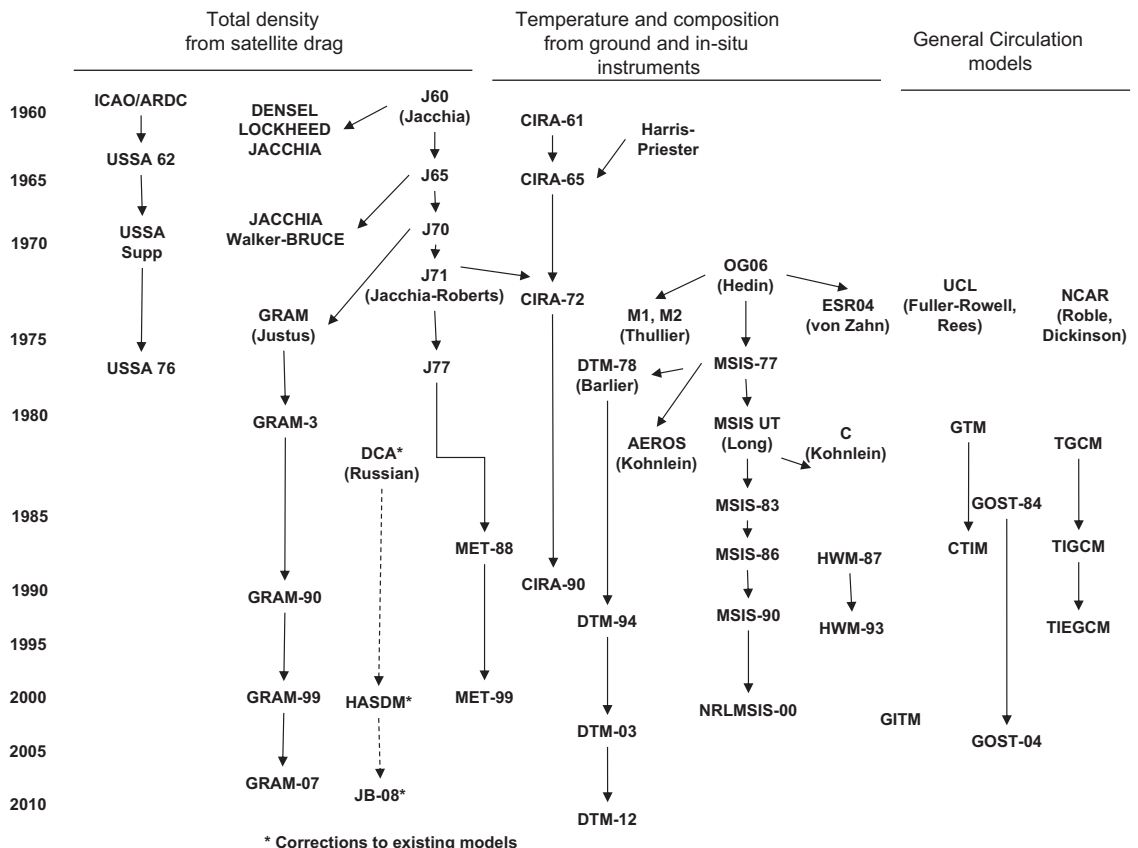


Fig. 3. Development of atmospheric models. Notice the variety of models. Flow of information among the three overall categories is limited ([14], 20). The main models in use today are the Standard Atmosphere, USSA76; variations of the Jacchia-Roberts, J71, J77, and GRAM99; COSPAR International Reference Atmosphere, CIRA90; Mass Spectrometer Incoherent Scatter, NRLMSIS-00; Drag Temperature Model (DTM), Marshall Engineering Thermosphere (MET), Global Ionosphere Thermosphere Model (GITM), the Russian GOST and general circulation models. Dynamic Calibration of the atmosphere (DCA) and High Accuracy Satellite Drag Model (HASDM) are corrections to other models, usually J70. The dashed line indicates that the concept for correcting the atmosphere followed the Russian work, but the models themselves are different.

probably more assumptions with atmospheric drag than with any other perturbing force used with satellites. We list some of the more obvious assumptions in this section.

- Assume $F_{10.7}$ is a suitable proxy for EUV which is actually believed to be the major factor in upper atmospheric heating [9]. Thuillier and Bruinsma [23] indicate the existence of a 13-day periodicity in EUV that is not represented in the $F_{10.7}$ data.
- The lower atmosphere rotates with the Earth.
- The sea-level atmosphere is composed of nitrogen (78.11%), oxygen (20.955%), argon (0.934%), helium (0.0006%), and hydrogen in “mixing to 105 km, and in diffusion above this height” [10]
- The change in mean molecular mass in the mixing region below 105 km is caused by oxygen disassociation [9]
- The shape of the temperature profiles remains constant with respect to basic models. Jacchia [10] said this is *a-priori* unlikely.

- The coefficient of drag equation is correct and complete as shown in Eq. (2).
- The atmospheric model precisely accounts for the variations in atmospheric drag including effects of diurnal variations, including the tilt of the Earth, the 27-day Solar cycle rotation, the 11 year solar cycle, semi-annual and seasonal variations, cyclical variations in the 11 solar cycle, upper atmosphere winds, magnetic storm variations, irregular short-periodic variations, tides, the proper altitude and spatial varying molecular components of the atmosphere, the appropriate lags for all factors affecting density, and other factors which may be as yet unknown.
- The precise method of employing the existing atmospheric indices is known and used
- All the input parameters (solar flux, geomagnetic indices (and any newer indices), atmospheric winds, distribution of molecular concentrations, etc) are available for historical, present, and future use. In addition their uncertainty is known with a certain precision into the future
- Any interpolation of the indices introduces no weak time dependence errors into the solution

- The proper times are used with each index, and any interpolation is matched to the actual time-varying behavior of the index
- The atmospheric model is appropriate for the orbital class of satellite under consideration

2.2. Indices

The complex interaction of the solar wind and the geomagnetic effects on the atmosphere might indicate a plethora of indices and expressions to properly model the total atmospheric drag effect. However, there are surprisingly few parameters in this category. Common parameters that have been used in model development to date include the following:

$F_{10.7}$, the Solar flux, many decades of values from <http://www.swpc.noaa.gov/Data/index.html>. This parameter originates in a similar region of the Sun where the EUV originates. Because EUV does not reach the ground, it has been used as a proxy for EUV. The data comes from two primary sources—Dominion Radio Astrophysical Observatory (DRAO) and Lenhart. The DRAO data is from the Penticton site in Canada. The Lenhart data comes from a reprocessing of the DRAO data.

$E_{10.7}$, only two days of data from http://www.spacewx.com/data/e107_nowcast.txt

S_{10} (from the SOHO satellite in a halo orbit at the L_1 Lagrange point since about December 1995),

Mg_{10} (from the NOAA and Nimbus satellites from 1978, [23]), “The Mg II core-to-wing ratio is derived from the

preferred geomagnetic index—MSIS uses a_p , Jacchia uses a_p or K_p but preferentially uses K_p . Others atmospheric models use K_p .

We note that the atmospheric models, in general, do not react instantaneously to an event occurring in either the solar flux or the geomagnetic index, but rather, they smooth the effect over a period of time.

Ultimately, the indices are a crucial step in determining the accuracy of any atmospheric model. If the variability of the parameter is greater than the effect it tries to model, the solution can become corrupted. We'll discuss the prediction aspect for these indices later, but this is another important limitation in the use of indices.

2.3. Available observational data

Development of atmospheric models is particularly challenging due to the complex interactions of atmospheric molecules, vehicle characteristics, solar environment, etc. It is further impeded by the non-availability of unclassified observational data for unclassified satellites. The US Air Force Joint Space Operations Center (JSPOC) often cites their unique advantage to access their observational database, but has refused to release any observations for independent verification of their claims, or for development of improved indices.

Historically, data was available, but very limited. The following atmospheric models list some of the data used in their development. The Jacchia models used sounding rockets (6 firings on Jan 24, 1967 from Cape Kennedy), and the following satellites

Name	Norad #	Period	Incl	Ap alt	Per alt	RCS	Launch/decay
EXPLORER 17 (S-6)	564	87.9	57.6	186	151	N/A	04/03/1963 to 11/24/1966
EXPLORER 32 (AE-B)	2183	87.5	64.5	162	140	0.4954	05/25/1966 to 02/22/1985
and compared to 5 satellites ECHO 2 (A-12)	740	94.5	81.4	522	465	N/A	01/25/1964 to 06/07/1969
EXPLORER 19 (ADI-1)	714	90.1	78.7	301	259	13.7332	12/19/1963 to 05/10/1981
EXPLORER 8	60	94.8	49.9	664	353	0.5910	11/03/1960
EXPLORER 1	4	88.5	33.1	215	183	N/A	02/01/1958 to 03/31/1970
INJUN 3	504	88.0	70.2	185	161	N/A	12/13/1962 to 08/25/1968

ratio of the h and k lines of the solar Mg II feature at 280 nm to the background or wings at approximately 278 nm and 282 nm. The h and k lines are variable chromospheric emissions while the background emissions are more stable. The result is a robust measure of chromospheric activity. The ratio is a good measure of solar UV and EUV emissions.” Thuillier and Bruinsma [23] show an approximate relation using the solar flux index. Mg II index = $0.000128F_{10.7} + 0.25068$.

ftp://ftp.ngdc.noaa.gov/STP/SOLAR_DATA/SOLAR_UV/NOAAMgII.dat.

a_p or K_p , for daily and planetary geomagnetic indices, data for many decades from <http://www.swpc.noaa.gov/Data/index.html>.

Most atmospheric models use the $F_{10.7}$, a_p , and K_p indices, primarily because they have been available for about 70 years. Some models are designed using a

The model development used least squares solutions and the satellites used $c_D=2.2$ below 300 km, which is a representative value across many approximations to aerodynamic drag. Jacchia mentions that $c_D=2.4$ might have been better, in which case the densities would be about 10% too high. The sample size is rather small, and the altitude dispersion is not too great. Also note that most of the Jacchia satellite data consisted of Baker-Nunn optical observations which are generally much less accurate than radar observations. The accuracy of this data is considerably less than what is currently available today—making it even more important to re-evaluate using today's modern radar measurements! It also highlights the fact that Jacchia models are often compared to modern models that were developed with modern data. However, the Jacchia models are operating over 50 years after the data from which they were formed!

The MSIS models generally used all the data available from the previous (Jacchia) models, plus “Barlier data, accelerometer data, and the atmospheric decay model data from the Jacchia models. (1) satellite drag [9,1,7], orbit determination (1961–1973); (2) accelerometer Atmosphere Explorer D, E) MESA Air Force SETA CACTUS San Marco 5; (3) incoherent scatter radar, exospheric temperature (Tex), Millstone Hill (1981–1997), Arecibo (1985–1995); (4) ISR, Lower thermospheric temperature (Tlow), Millstone Hill (1988–1997); (5) Solar Maximum Mission (SMM) O2 density data derived from occultation of solar UV emissions.” [17] Notice the large increase in available data!

Today, there are additional sources of data with which to develop atmospheric drag models. Satellite Laser Ranging Data (SLR) exists for many satellites, and GPS and accelerometer data are available from some sources. However, obtaining these data at the same time a Precise Orbit Ephemeris (POE) is developed and available becomes difficult. In the absence of raw observational data, one can also use the POE itself as a data source—an option we use later. This requires that the POE be long enough that you could get a “converged” solution from an independent orbit determination and still have enough data to perform a comparison with. The absence of maneuvers is also desirable.

2.4. Orbital classes involved in model formation

The early researchers had few observations to work with, and there weren't very many satellites in orbit (compared to today), or enough orbital classes (a variety of orbital inclinations within about 1500 km altitude) to ensure adequate and global coverage. As a result, many of the early models were very limited in their ability to generically represent atmospheric drag over a variety of orbital inclinations and altitudes.

We cite an example from J70. The Jacchia models (J70) state a range of altitudes from 90–2500 km, but the paper states that above 1100 km there was no reliable observational data (as is seen from the available satellite data), and all the results were simple extrapolations [9]. The overall technique is analogous to the gravity field tuning that is sometimes done for precise orbit determination applications—although here the tuning limits the applicability to all orbital regimes.

Despite these limitations, researchers were able to assemble models that are still relevant today. The limitation from available data is still present in some current atmospheric models. Doornbos [3] found that during 2003, NRLMSIS did as well or better than JB2006 for a satellite at 800 km. On the other hand, JB2006 and JB2008 better represented the variance of CHAMP and GRACE accelerometer data (through 2009) by 1 to 4%. Because time dynamics are clearly a factor in such comparisons, we wonder how JB2008 (and MSIS et al.) perform outside of the timespans over which they were fit to the input data.

2.5. Fidelity

The previous discussion of assumptions, data etc. produce a wide range of accuracy for the atmospheric models. Numerous studies ([9,10] is one example) find that no single

atmospheric model is conclusively better in all applications for all satellites, and this makes sense given the limitations of the indices and the available satellite data.

Often, a program simply uses the available models that were programmed long ago. Implementing new models is difficult due to many older computer programming styles and practices, and so it's often easier to use the old models that already exist. For example, the JSPOC still primarily uses a version of Jacchia 70 despite several advances noted in the development of newer and more modern methods (J71, NRLMSISE-00, DTM-12, etc).

3. Atmospheric model use

3.1. Indices

Most models use the $F_{10.7}$, K_p/a_p parameters because they are available for the longest period of time. In fact, $F_{10.7}$ measurements have been made since the 1930s. Some of the newer indices are available only after the satellite was launched (1995, etc), while others must be purchased, or are even classified. This limits the period of time for analysis to older data and for independent verification, but it is still relevant.

Not often discussed is the accuracy of the measurement indices. Each measurement has an uncertainty, but this is virtually never addressed. Coupled with this fact is the missing data points which occur occasionally. The Sun hasn't gone out for a day, but there are cases, usually in the past, where zero solar flux values are reported. The data points are corrected for those cases in the EOP and Space Weather files on CelesTrak (<http://www.celestak.com/SpaceData/>) by doing a simple linear interpolation between the adjacent points. As a minimum, this should mitigate the impact of having a zero input.

To further complicate the accuracy issue, there are **observed** and **adjusted** values for some of the parameters—a process that adjusts the value to one that would be recorded at an average Earth-Sun distance, or to simply use the observed value that varies during the course of the year due to the Earth's distance and orientation from the Sun. The process to convert between values is in Eq (4) where AU is simply the distance to the Sun in km.

$$F_{10.7(obs)} = \frac{F_{10.7(adj)}AU^2}{r_{K-L}^2} \quad (4)$$

The published data does not always match Eq. (4) (see Fig. 4), and the differences can be quite large.

Jacchia and most other atmospheric models use the adjusted values, published by NGDC: ftp://ftp.ngdc.noaa.gov/STP/GEOMAGNETIC_DATA/INDICES/KP_AP/

MSIS expects to use the actual observed data, and not the adjusted value at 1.0 AU. ftp://ftp.ngdc.noaa.gov/STP/SOLAR_DATA/SOLAR_RADIO/FLUX/DAILYPLT.OBS

Gathering the data for a program can be challenging. [24,25] developed a process to automatically combine the several sources of data into a single file that is constantly updated to produce the current historical and predicted values. CelesTrak provides this resource. The files are

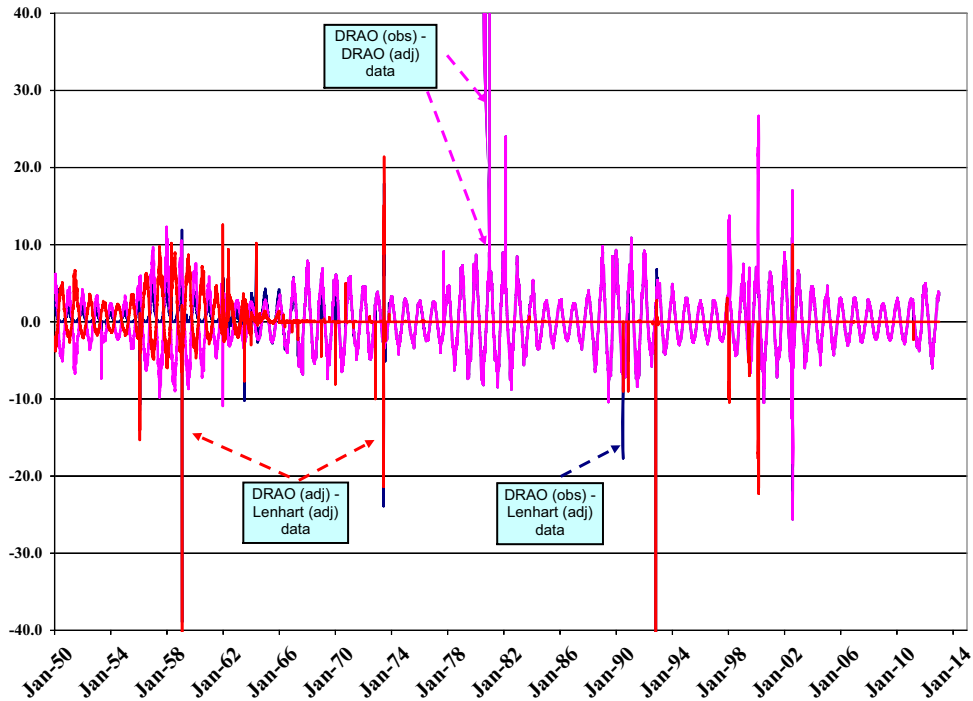


Fig. 4. Difference of observed and adjusted solar flux values. The solar cycles are evident in the observed minus adjusted solar flux differences, along with the seasonal variations that drive the original variations over time. The data spikes occur in both observed and adjusted values, and in the DRAO and Lenhart data for a variety of reasons including [erroneous] multiple Sun–Earth distance corrections.

updated continuously, and are completely free for use. Documentation is included on the assembly. This single format is very useful for operational programs needing constant updates as they are published, but not wishing to expend the resources to assemble the data.

The primary quantity, $F_{10.7}$, has been used as a proxy for the EUV radiation for many years. Several new indices have been under consideration for the past few years – Mg II (from NOAA and other satellites at about 280 nm), EUV (from the NASA/ESA SOHO satellite at the Lagrange point at 26–34 nm), etc. – but none has been unequivocally proven better than another and established as a new leader that will dramatically improve the accuracy of satellite operations. New parameters have begun to appear with the advent of satellite based sensors. Some of these data are available (some must be purchased) from the Space Environment website.

<http://www.spacewx.com/index.html>

Many of the newer indices are available only back to 1997, they lag the current time by about a month, and they contain no predictions. The data has the observed $F_{10.7}$, centered 81-day average, S_{10} , S_{10} 81-day centered average, Mg_{10} , Mg_{10} 81-day centered average, Ssrc. There are several costs, and registrations for some of these, and update intervals are sometimes limited to researchers outside the US Air Force.

3.2. Predicting solar flux

Solar flux receives a lot of attention because it is an important parameter in determining atmospheric density. Moreover, predicting the $F_{10.7}$ values into the future poses

significant challenges, and introduces significant uncertainty into operations requiring accurate forecasts of atmospheric behavior. Schatten and Sofia [20] produces a monthly estimate of $F_{10.7}$ and a_p . Notice the dramatic changes during the course of a single solar cycle Fig. 5.

Fig. 6 examines a shorter span of time and current data. The variability of the predictions is readily apparent. Most predictions rely on the solar sunspot activity. This has been routinely monitored since the 1700s. A relation exists between the sunspot number, R , averaged over a month or longer, and $F_{10.7}$.

$$F_{10.7} = 63.7 + 0.728R + 0.00089R^2 \quad (5)$$

The polynomial trend (Eq. (6)) is intended only to match the last few solar cycles, assuming the next will not change dramatically from the previous. In Eq. (6), t is the number of days from January 1, 1981.

$$F_{10.7} = 145 + 75 \cos(0.001696t) + 0.35 \sin(0.00001695t) \quad (6)$$

While no claim is made to its' accuracy, it offers an alternative for programs requiring some estimate of solar flux into the future. The best course of action is to design for a more rigorous solar flux period, and if the actual is much less, the lifetime of the satellite will likely be longer. Fine tuning the fuel budget based on an overly conservative solar flux estimate could shorten satellite lifetime unnecessarily.

The predictions also come with early, middle, and late values. These account for cycles that are either early or late. Fig. 7 shows a sample from 1995 for Cycle 23. Notice

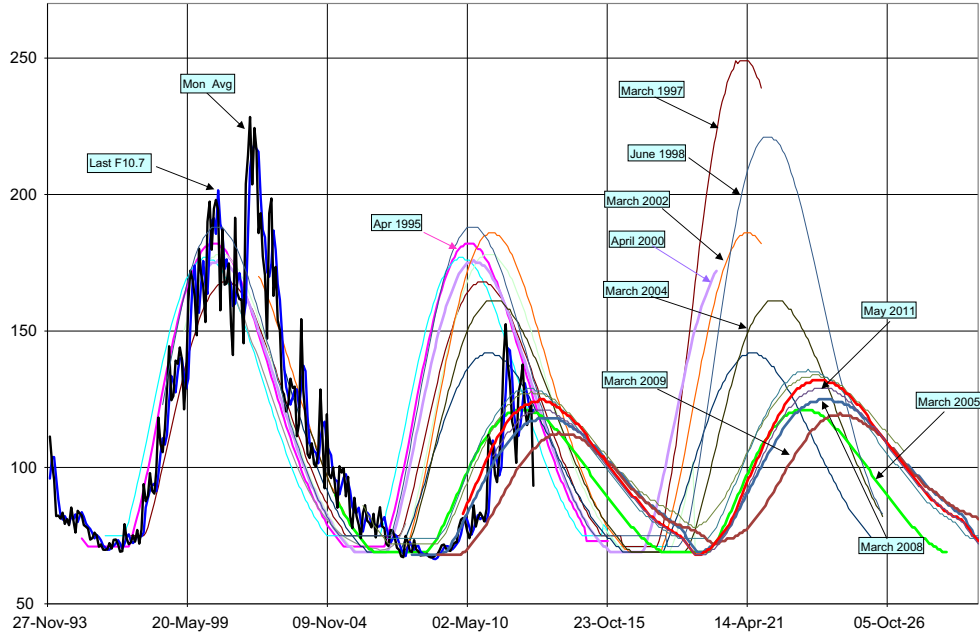


Fig. 5. Recent solar flux predictions. Several Schatten predictions of solar flux are shown along with the polynomial trend. Notice that each Schatten prediction covers about two solar cycles and the latest predictions suggest a lower solar max for cycles 24 and 25. Predictions just one solar cycle apart can differ by more than the total increase in solar max (e.g. Mar 97 and Mar 07).

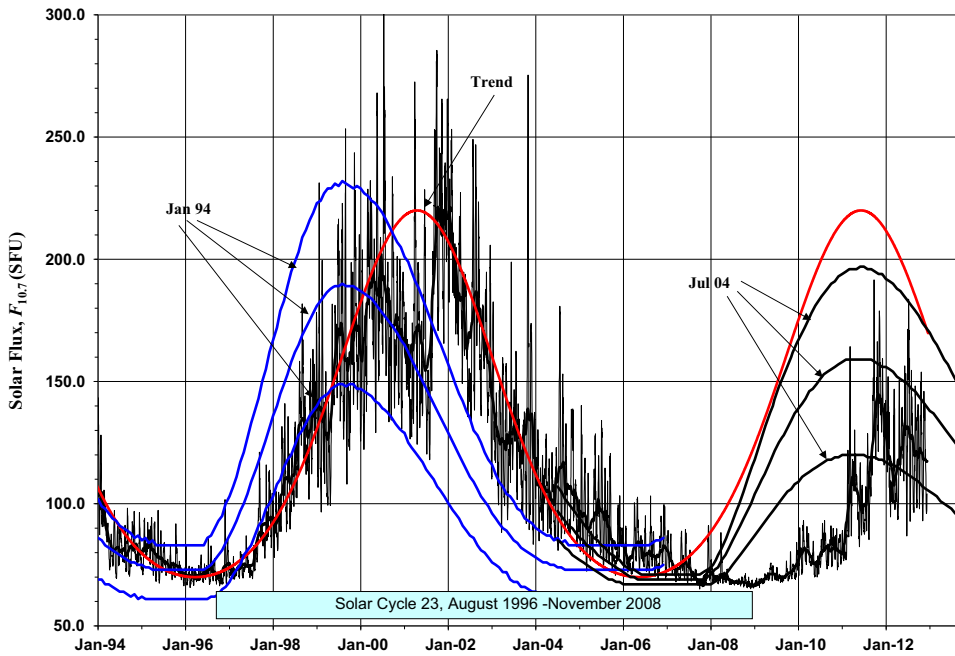


Fig. 6. Recent solar flux predictions. Two Schatten predictions of solar flux are shown along with the polynomial trend. Notice that each Schatten prediction has a minimum, medium, and maximum prediction that vary quite a bit. They also suggest a lower solar max for cycles 24 and 25.

that both the middle and the late predictions were accurate for portions of the Cycle, but the next cycle was completely missed by all the predictions.

Recognize that these predictions are long-term. To properly determine the 81-day averages for a practical orbit propagation scenario, one needs the detailed predictions for 50–60 days in advance (depending of course on the length

of the propagation). The NOAA website (<http://www.swpc.noaa.gov/Data/index.html>) provides 27 and 45 day predictions which are incorporated in the Celestrak data files. These can be used to extend the space weather data, but they introduce significant error Fig. 8.

A review of the 45-day forecasts of $F_{10.7}$ and a_p , which comes out daily, let us evaluate the prediction accuracy. For

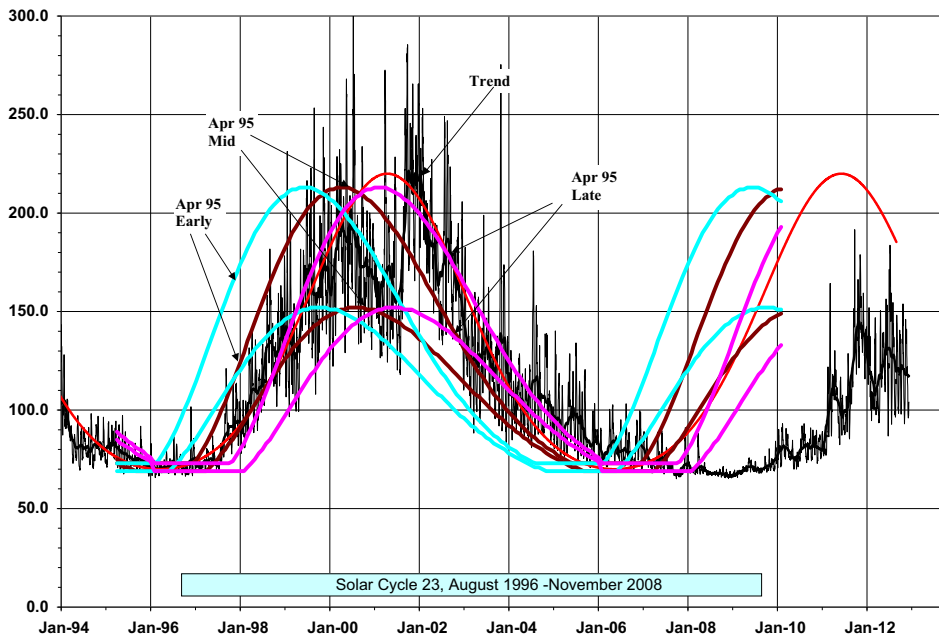


Fig. 7. Solar flux predictions for early and late cycles. Schatten predictions of solar flux are shown for cycle 23. The early and late predictions attempt to accommodate longer cycles such as Cycle 23. For this cycle, it appeared that the late prediction was better, although it missed the average maximum value by almost 40 SFU and did not adequately predict the span of the cycle.

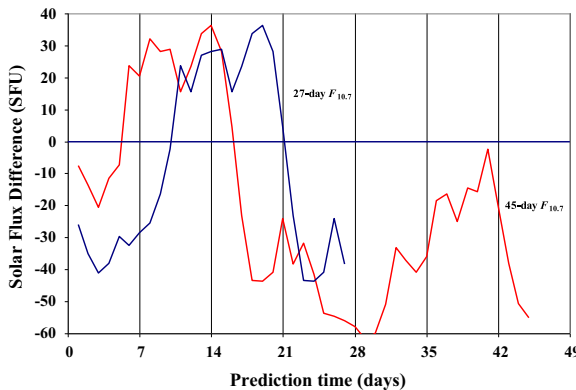


Fig. 8. 27 and 45 day prediction values. Notice the large swings in the predicted and actual indices. Solar storms can cause differences of more than ± 40 SFU on any day.

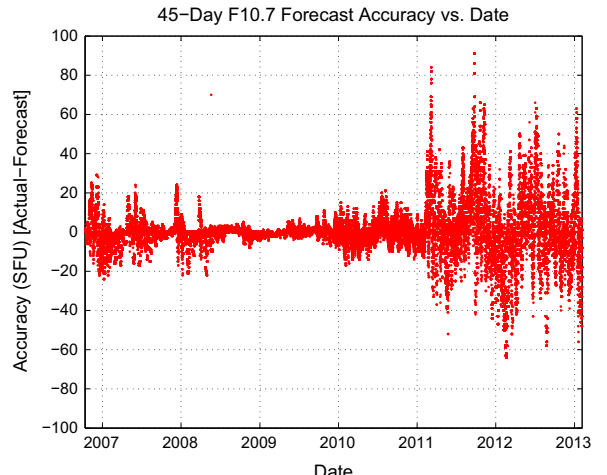


Fig. 9. Accuracy of 45 day $F_{10.7}$ prediction values. Predicted values are compared to actual values on each day. Notice that the predictions are better during solar minima around 2009.

both $F_{10.7}$ and a_p , we took the 45 day forecasts for each data type and compared to the actual data on those days. Fig. 9 is for $F_{10.7}$ and it shows the accuracy for each date's 45 forecasts over the span of our archives (2007–present). As expected, the forecasts are generally good around solar minimum but show a lot of variability around solar maximum. Still, almost all of the data is within ± 20 –40 SFU.

Fig. 10 shows the accuracy of the predictions plotted against the prediction interval as a contour plot. Most of the data predicts well, with the majority of the predictions within a couple of percent of the observed results. But there can be large outliers even for short prediction intervals. As expected, as the forecast interval increases the variance increases, as well, and the contours flatten out.

For the a_p forecasts, Fig. 11 shows the spread of the 45 forecasts for each date over the period 2007–present. Here the results are presented as the difference between the average for that date and the forecast, measured in gammas. Somewhat surprisingly, there is not as much variability over time, but there is a clear bias (forecast values are greater than the actual observations).

The contour plot for the a_p forecasts shows little variability in the quality of the forecasts with prediction interval and clearly shows the bias between predicted and observed values Fig. 12.

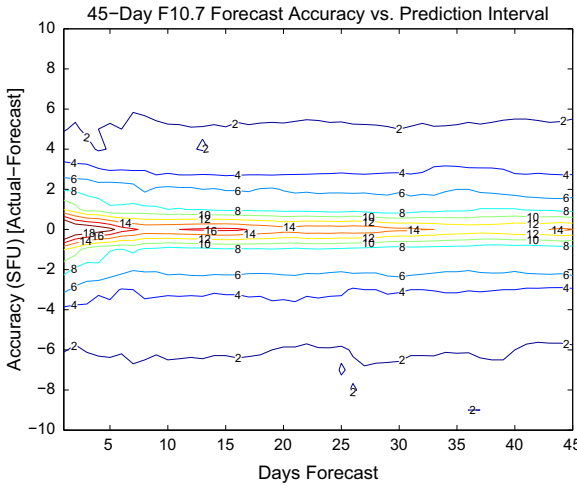


Fig. 10. Accuracy of 45 day $F_{10.7}$ prediction values. The percent accuracy of the predicted values are shown from the epoch time. Errors in the predicted values are less than about 1 SFU only about 5–10% of the time.

As part of their work to maintain and conduct mission operations for the European Space Agency (ESA), the European Space Operations Center (ESOC) has developed a prediction service for solar flux. ESOC uses *Prediction of Flux and Ap* (PDFLAP) (for short-term forecasts) and (*SOLMAG*) (for long-term forecasts). The programs were developed in the 1990s by the British Geomagnetic Service BGS/Edinburg under ESA management PDFLAP looks at the traditional $F_{10.7}$ daily values and the daily a_p indices, for about one solar rotation period in advance. The resulting indices are then used with MSIS-like atmospheric models, and the results indicate they perform quite well with observational data. The ESA Space Debris Office have embedded PDFLAP and SOLMAG in automated programs to upload recent NOAA data, perform daily short-term forecasts, and to calculate long-term forecasts each month.

Oltrogge and Chao [16] extrapolate and interpolate atmospheric density based on adjusting or modifying the density values, not the proxies. The rationale is that the dependence of density on the proxies is nonlinear; hence averaging or interpolating proxies does not yield correct average or interpolated density. They were examining the effect of solar flux prediction estimates on satellite lifetimes and noted that most orbit lifetime prediction errors were caused by (1) the unreliability of current ‘mean’ solar activity predictions as compared to actual activity variations; (2) non-availability of predictions more than one solar cycle away; and (3) nonlinear density as a function of solar and geomagnetic activity. To circumvent these obstacles, they used the complete set of solar and geomagnetic data available (from Feb 1947). Thus, five solar cycles were used and combined into a single cycle of 10.82546 years (3954 days). Rather than attempting to produce a single mean solar cycle, they chose to directly use the solar flux and geomagnetic values from the previous cycles. Essentially, the technique creates a day of solar and geomagnetic data (a combined triad of values including the $F_{10.7}$ 81-day average) from one of the five cycles at random, and does so for each day of the simulation. Thus, the existing data is used to construct a future solar cycle, while retaining all

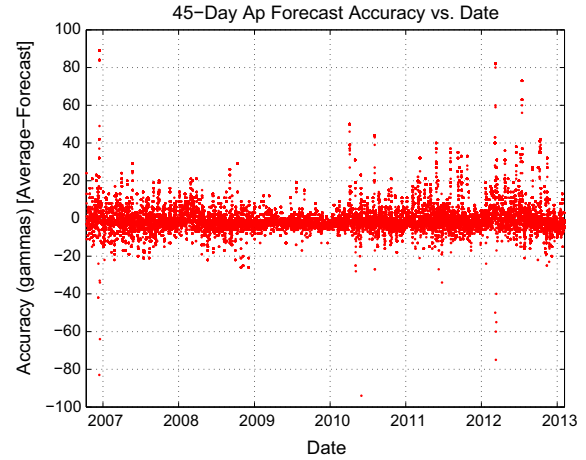


Fig. 11. 45 day a_p prediction values. The accuracy of the predicted values are shown on each date. Errors in the predicted values are generally less than about 20 gammas. There is a slight negative bias.

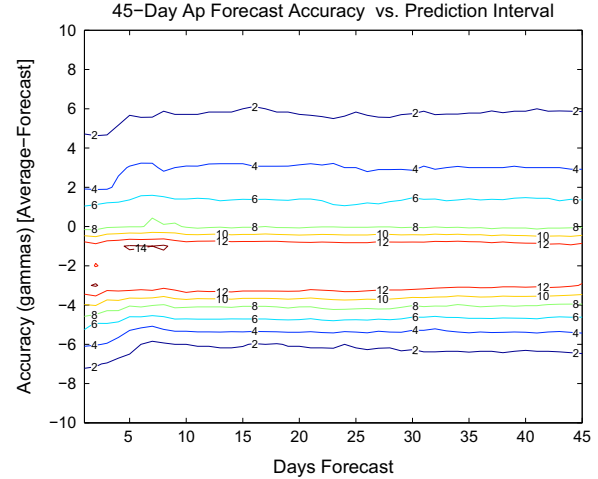


Fig. 12. 45 day a_p prediction values. The percent accuracy of the predicted values are shown from the epoch time. Errors in the predicted values are less than about 1 gamma only about 5–10% of the time. Also notice the slight negative bias of about 2 gammas in all the predicted values.

the variability and interrelations of the existing data. Their resulting solar and geomagnetic activity computer code ‘tdt2f10ap_60 yr’ is available upon request from the author (Oltrogge@1EarthResearch.com) for users wishing to explore the model in greater detail. This technique is certainly worthy of additional analysis and use as it avoids the vagaries of other prediction techniques that appear to vary widely over just a single solar cycle.

The bottom line for prediction is that it arguably represents one of the largest contributing factors to differences in atmospheric modeling. Solar flux can easily vary by 30–50 SFU which, and as we will see in Fig. 14 (the constant cases), represents a difference of about 1 to 10 km. Not including the proper geomagnetic indices (the adjusted daily case), also from Fig. 14, indicates a potential for differences of about the same amount. Furthermore, if a satellite was designed in 1994 with then

available predictions, its lifetime would be significantly different one solar cycle later as the new estimates for the next solar max are nearly 120–150 SFU less than the previous. This represents a difference as large as the mean solar max to solar min difference. Of course, here the estimate was downward, and satellite lifetime would likely be lengthened. However, a prediction that was too low would have dramatic differences on satellite lifetime.

3.3. To interpolate or not?

The question evokes considerable discussion and is usually centered on the geomagnetic indices, but also applies to the solar flux and other parameters. Some models (NRLMSISE-00 for instance) suggest that they were developed to use the step-function values of the 3-hourly geomagnetic indices [17], although they did use the daily a_p during “quiet” periods ($a_p < 10$) and then switched to the 3-hourly a_p during “active” periods ($a_p > 50$). Because the space weather data is provided at discrete time intervals, it’s reasonable to imagine that one should interpolate the indices to provide a smooth data input. This causes two problems. First, some researchers do not feel that interpolation should be done due to the original definitions of the models. Some models state that they were developed for use without any interpolation. Notwithstanding these statements, nature seldom operates in a digital fashion, rather operating in a continuous analog manner. The rates of change can be quite rapid, but common sense indicates a continuous representation should better replicate the actual environmental conditions under consideration.

To further support the idea that interpolation is all but required for atmospheric models, consider the mathematical processing of a model such as the Jacchia models. Every parameter, temperature, and density is formulated with a polynomial to represent the tabular observed or calculated parameters. If continuous functions are necessary (sufficient) for these parameters, they should be for the input indices as well. Jacchia ([10]:38) states “all these equations give only a smoothed version of the real variations, for which no model exists ... Even in this case, however, the formulas should not be used with the original 3-hourly K_p indexes but rather with a smoothed K_p index in which the smoothing is commensurate with the resolution of the observed data”. Tanygin and Wright [22] showed how not interpolating the input parameters caused a failure of the McReynolds Filter-Smooth test.

We conclude the need for interpolation, but which method of interpolation? Vallado [27]:558–560 shows a cubic spline interpolation that recovers the data at each measured point. This should be adequate for most applications. However, be aware of the differences that alternate interpolation techniques can insert into the propagation or orbit determination results.

We summarize our current understanding of the possibilities:

- K_p is a set of discrete categories defined by Chapman and Bartels (1940). As such, they should not be

interpolated. In addition, atmospheric models should ideally use a_p as the input because it affords additional sensitivity not available in the K_p scale.

- a_p values should be interpolated. The cubic spline approach discussed in Vallado and Kelso [24] is recommended.
- For models using the K_p index, the ideal method of operation is to interpolate the a_p values, and then select the discrete K_p value. However, this is not usually feasible, thus interpolation of K_p is an acceptable variation.
- Programs should strive to use the newer Northern and Southern geomagnetic proxies (a_n and a_s respectively) as they represent a more rigorous approach. The older a_p values are still valid for historical continuity.
- The options for using a_p or K_p (and $F_{10.7}$) should be:
 - Daily: Just the daily values are used without interpolation. All 3-hourly values are ignored.
 - 3-hourly: Just the 3-hourly values are used. The daily values are ignored and there is no interpolation. This will produce step function discontinuities for both solar flux and geomagnetic values.
 - 3-hourly interp: This could use the cubic splines, but may use other interpolation techniques. It should produce the smooth transitions from one time to the next while preserving the discrete values. The measurements should reproduce exactly at the measurement times (e.g., 0000, 0300, 0600 UTC), and be smooth in between. Both solar flux and geomagnetic values are interpolated.

3.4. Timing

Most atmospheric models use a 3-solar rotation (81-day) average for the solar flux. The technical descriptions usually specify a centered 81-day average. However, this presents a practical difficulty as the predicted values of space weather parameters are not particularly well known. Thus, programs should have an option to use either the last $F_{10.7}$ 81-day average, or the centered 81-day average. The differences can be quite large depending on which approach is used. Most atmospheric density model descriptions generally cite a centered average.

The time of the space weather measurements are also relevant, particularly the solar flux. Program codes should treat all $F_{10.7}$ measurements at the time the measurement is actually taken. The time (20:00 UTC after 1991 May 31, 17:00 UTC before) should be used with all $F_{10.7}$ and average $F_{10.7}$ values. Any model specific “day before,” “6.7 h before,” etc., should reference this time. This can be a km-level effect. Note that some organizations may not use these time constraints, and therefore require a different time offset. It’s not a good idea to introduce unnecessary confusion by ignoring the reality of a timed observation.

There is also a time lag for the density to increase after a particular event. There are two components. First, the atmospheric model response to a rapid change in solar indices, and second, the time lag before the density will increase. For the first case, consider a sudden change in the solar flux. Each atmospheric model will respond differently, but none will immediately change the density for

the current time as the atmospheric models do not respond that fast to individual changes in indices. You can see this by the use of an 81-day average in the equations. This is somewhat related to the second effect where different atmospheric models can experience a difference in how long they take to “register” an effect. Usually, this is associated with the diurnal aspect where there is about a 6 h lag after the atmosphere is exposed to the Sun and until the daylight begins a noticeable effect on the density. Thus, the a_p (K_p) lag values are fixed to values such as 6.7 h, but other times have been proposed. Software should accommodate future changes to lag times without the need to re-compile.

3.5. Tests

A series of tests were run to determine the variability of different atmospheric models for a given satellite using a single software analysis program, and the differences resulting from the treatment of the input solar weather data. The state vectors, epoch, BC, and solar radiation pressure coefficient ($m/c_r A_{\text{sun}}$) were held constant for all runs. The baseline used the Jacchia–Roberts atmospheric model. The simulations were run during a time of “average” solar flux (January 4, 2003, $F_{10.7} \sim 140$). Minimum solar flux periods ($F_{10.7} \sim 70$) would show little difference. Maximum periods ($F_{10.7} \sim 220$) would show much larger excursions. Fig. 13 shows the results for a notional JERS (NORAD satellite #21867 in a Sun synchronous about 600 km altitude orbit). Additional runs were performed with different satellites and as expected, the results were larger for lower and more eccentric orbits.

If we select a single atmospheric model, Jacchia–Roberts–71 for instance, we can also evaluate how the propagation is affected by treating the data differently. We chose some generic parameters because this is only a simulated case. The cases use either the daily geomagnetic values (Dly), the 3-hourly values with no interpolation (3Hr), or the 3-hourly values with spline (3HrSpl) and polynomial interpolations (3HrInt). The observed and adjusted parameters were also tested (obs vs adj). Finally, we also looked at holding all the values constant (ConAll and (ConAllAvg).

From Fig. 14, note that simply changing the solar flux to be a constant – a difference of only a few SFU's – causes nearly a 10 km difference at 4 days (yet we saw earlier that predictions (long and short) can result in Solar Flux changes of 30–50 SFU's!). This indicates that the prediction of solar flux is very important, and if it differs by more than just a few SFU's, can have dramatic effects on the results of a propagation. The important point to understand from Figs. 13 and 14 is that the choice of atmospheric model has as much effect on the overall results as the various ways to use the input data. This is remarkable as many organizations “go to the mat” for a particular model. However, based on how they use the input data parameters, they may actually obtain worse results than had they simply used the input parameters differently!

To summarize, the major error sources for atmospheric model use in using atmospheric models are listed below (note that density, BC, etc., are not listed as they are

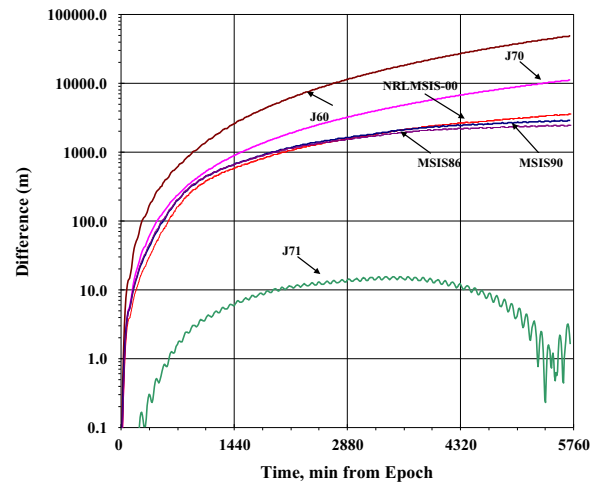


Fig. 13. Sample atmospheric drag sensitivity: Positional differences are shown for satellite 21867. Jacchia–Roberts atmosphere is the baseline for all runs using 3-hourly geomagnetic values. The graph shows the propagation variations by simply selecting different atmospheric models.

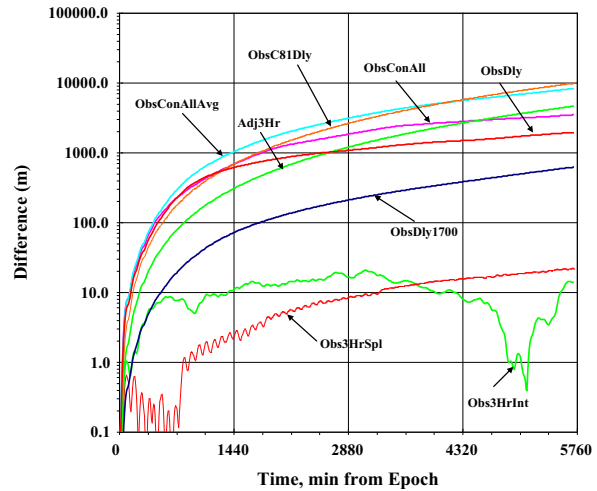


Fig. 14. Sample atmospheric drag sensitivity: Positional differences are shown for satellite 21867. Jacchia–Roberts is the baseline for all runs using 3-hourly geomagnetic values. The graph shows the effect of various options for treating solar weather data. Specific options are discussed in the text. Note that the scale is the same as Fig. 13, the relative effect of different models and solar data options are about the same, and any transient effects quickly disappear as the overall effect of drag overwhelms the contributions.

derivative effects from the items listed below). This list is generally ordered in decreasing magnitude of effect, although the exact effect will differ with different orbital regimes and solar conditions.

- Using predicted values of $F_{10.7}$, K_p , a_p for real-time operations
- Lack of satellite attitude in determining the time-varying cross-sectional area
- Not using the actual measurement time for the values ($F_{10.7}$ in particular at 2000 UTC)

- Using step functions for the atmospheric parameters vs interpolation
- Using the last 81-day average $F_{10.7}$ vs. the central 81-day average
- Using observed or adjusted space weather parameter values
- Using undocumented differences from the original atmospheric model technical definition
- Not accounting for [possibly] known dynamic effects—changing attitude, molecular interaction with the satellite materials, etc.
- Inherent limitations of the atmospheric models
- Use of differing interpolation techniques for the atmospheric parameters
- Using approximations for the satellite altitude, solar position, etc.
- Using a_p or K_p and converting between these values
- Use of $E_{10.7}$ vs $F_{10.7}$ in the atmospheric models (this is not well characterized yet)

4. Satellite parameters

4.1. Mass

Satellite mass is probably the easiest parameter to choose/set in calculations because it is either known by the owner operator, is constant because there is no thrusting capability on the satellite, or is unknown because the data is not released. The latter category presents additional difficulties and will not be considered directly here, noting that the general case for which satellite information is not known is handled via a solution in which the entire ballistic coefficient (BC) is solved as a free parameter.

4.2. Coefficient of drag

The coefficient of drag was investigated in the early 1960s ([13,21], etc.) and tested mainly for use in the developing ICBM programs. Some work continued but not much work applied to satellites. Gaposchkin [4] assembled a wealth of information about the early research, and coupled it with his own knowledge and research into atmospheric drag. He summarizes many things:

- c_D The coefficient of drag is related to the shape, but ultimately a difficult parameter to define. Gaposchkin [4] discusses that the c_D is affected by a complex interaction of reflection, molecular content, attitude, etc. It will vary, but typically not very much as the satellite materials usually remain constant.
- Plots of c_D vs altitude are important. From the historical literature, note the limited altitudes in the plots. One could assume the graphs increase without changing, but the very nature of c_D and its interaction of materials plus atmospheric constituents suggest that may be an incorrect assumption Fig. 15.

Graziano [6] examined the principal approaches to modeling aerodynamic drag across the low Earth orbit regime. Fig. 16 [13] delineates the major approaches to

determining aerodynamic drag across low Earth orbit altitudes (or correspondingly large ratios of mean free path to satellite characteristic dimensions). Note that a single static value is not even shown.

The key discriminator is the magnitude of random, thermal velocities relative to the bulk velocity of the atmosphere, or equivalently, the orbital velocity of the satellite. In the hyperthermal regime, random motion is small compared to bulk directed velocity. This exists over much of the low Earth orbit regime. Continuum flow in which thermal velocities are large compared with directed motion applies only at very low altitudes, calling further in question use of the simple drag formula. However, the ratio of thermal speed to bulk velocity does not vary monotonically with altitude.

At higher altitudes, the residual atmospheric gases separate into strata according to molecular mass. Gaskinetic temperatures increase with altitude due to absorption of highly energetic solar radiation by the small amount of residual oxygen. Temperatures are highly dependent on solar activity. The few particles of gas in this area can reach 2500 °C (4532 °F) during the day. Actually, the random velocities of gas particles can be greater than the orbital velocity, because the statistical definition of temperature fails. This region is called the thermosphere. It begins about 90 km above the earth. The upper reaches of the near Earth orbit regime may be sub-hyperthermal. Marcos et al. [15] and others have reported thermospheric cooling, which impacts orbit lifetime for many satellites.

Panel methods decompose the spacecraft into discrete flat facets and model the interaction of gas particles with the surface. The Ray Tracing Panel (RTP) method follows the trajectories of scattered particles so that collisions with other satellite surfaces may be included. Test Particle Monte Carlo (TMPC) approaches fire aggregates of many molecules at the surface with like characteristics upon which a drifting Maxwellian distribution is imposed. This also accounts for multiple encounters with satellite surfaces but not of particles with each other. The most widely applicable approach is Direct Simulation Monte Carlo (DSMC) in which the laws of physics are applied to a statistically significant number of individual particles. The particles can interact with each other according to a prescribed interparticle potential function, which includes elastic collisions. The particles can exchange momentum and energy (including that in internal degrees of freedom) with each other and

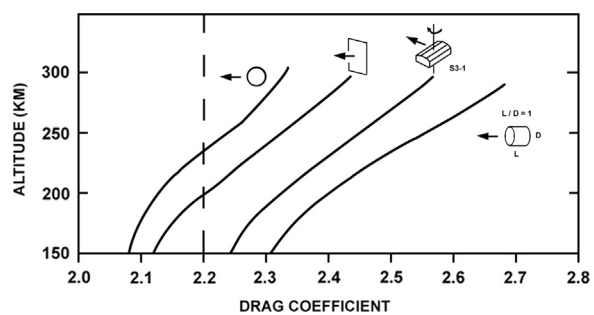


Fig. 15. Coefficient of drag values. Sample c_D values from Sentman [21]. There is a practical limit of values between 2.0 and 4.0, but operationally, much higher values are possible.

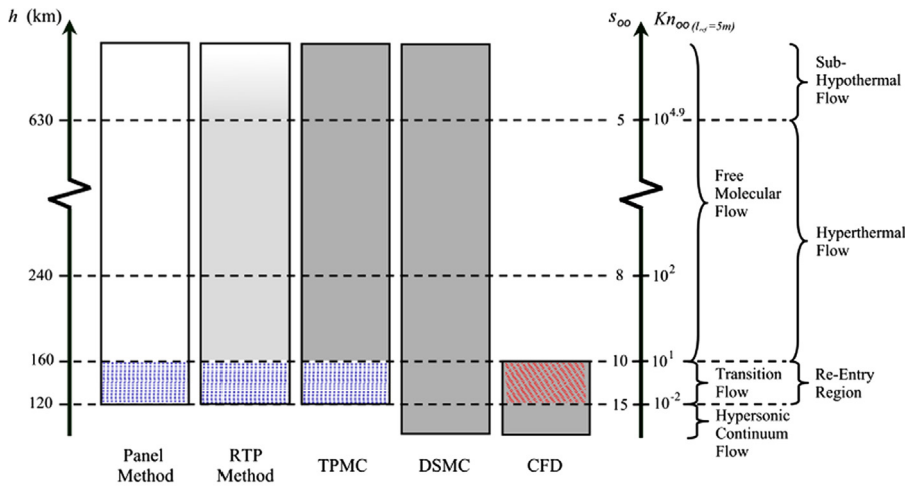


Fig. 16. Approaches to solving the coefficient of drag. Several approaches are shown against altitude with the most accurate techniques on the right. Graziano [12].

with the surface. Computer Fluid Dynamics (CFD) includes a spectrum of mathematical and numerical techniques to solve the continuum Navier–Stokes equations, the existence of individual particles need not be considered.

All of these techniques require hypotheses about the interaction of the gas with solid surfaces. For example, in profound continuum at low altitudes, the gas is assumed to “stick” to each surface. There can be no relative motion between the surface and the gas next to it. When the medium is less dense, there can be slip between the gas and the surface. The surface interaction depends on the degree to which the gas “accommodates” to surface conditions. The accommodation coefficients depend on the surface material and the condition of the surface, for example, the scale of surface roughness. These properties vary widely among materials and with the events that a surface experiences during its lifetime. Gas particles might adhere to a surface during flight, or the surface might grow hot, and its surface characteristics change during its mission lifetime. Gaposchkin [4], among others, explain most used approaches to determining aerodynamic forces in rarefied flows including surface accommodation characteristics. Ultimately there is great uncertainty.

The simulations in Fig. 17 illustrate the variation of predicted drag with velocity, altitude, and surface characteristics. We chose a warm surface as though it were heated by the Sun. Note that the drag coefficient is not 2.2, as commonly assumed, but it is in the range 2–4 predicted by the simple continuum formula.

It is very important that density, temperature, and Mach number cannot strictly be defined under such rarefied conditions. Drag does not necessarily scale as velocity squared or linearly with area. For example, there is little difference between a circular disc with finite area and a vertical flat plate with infinite or undefined area because there are few collisions between particles that have encountered the surface either with each other or with the oncoming flow. It is better that one calculate the relevant forces and moments and employ them directly.

This is what the most comprehensive operational analyses do. The ESTEC model suite developed by Fritzsche and others, exemplifies complex, careful analysis of aerodynamic (and radiation induced) forces on satellites [23]. The ESTEC Rarefied Aerodynamic Modeling System for Earth Satellites (RAMSES) model uses the TPMC approach and accommodates surface shadowing. Klinkrad and Fritzsche [11] have used RAMSES incorporated in the more comprehensive Analysis of Non-Gravitational Accelerations due to Radiation and Aerodynamics (ANGARA) formalism for radiation and kinetic momentum transfer to estimate forces and moments on ERS-1 and ENVISAT. The magnitudes of the forces are consistent with previous estimates in this paper, on the order of 10^{-5} N t.

4.3. Area

The satellite area can be easy to determine (spherical shape or constant area to the velocity vector), or complex (all others). The easy case is very common within the context of the entire satellite catalog, but it nevertheless provides opportunities to investigate the variability of the other parameters. Clearly, the shapes of various satellites are not spherical—with the exception of a few calibration spheres. Notice the shapes of the satellites in Fig. 18.

The cross sectional area changes constantly (unless there is precise attitude control, or the satellite is a sphere). This variable can change by a factor of 10 or more depending on the specific satellite configuration. Macro models are often used for modeling solar pressure accelerations, but seldom if ever, for atmospheric drag.

The most technically accurate approach is to input the attitude (quaternions, direction cosines, etc) into the orbit determination solution and simply account for the actual or predicted attitude, and thus the actual frontal area exposed in the relative velocity direction. Very few programs are able to accomplish this.

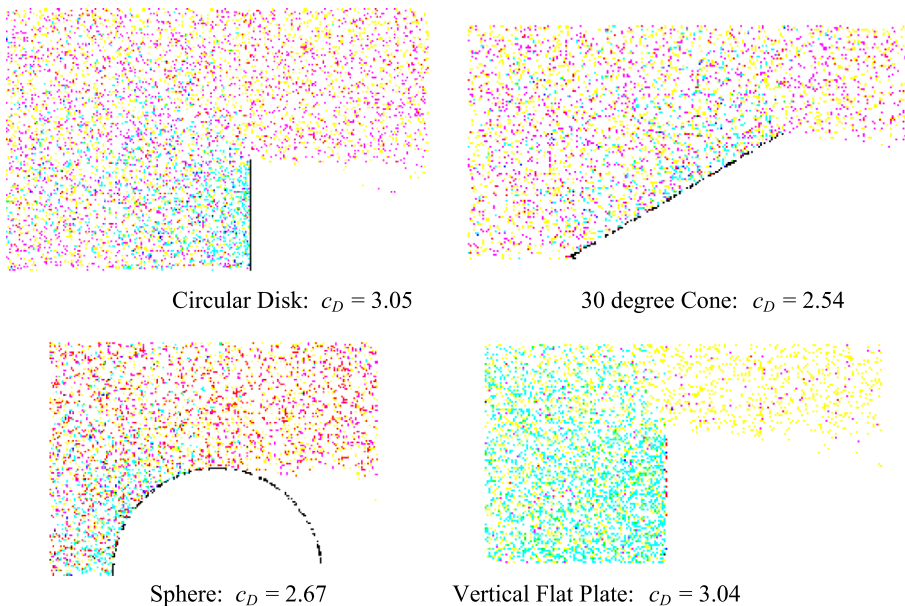


Fig. 17. DSMC simulations, $M=10$, $K_n=1000$, 10 collisions required for relaxation of internal degrees of freedom, surface temperature=free stream stagnation temperature. Red particles are unaffected by the presence of the sphere. Blue particles have collided only with the surface. Yellow particles have experienced multiple interparticle collisions. All objects have the same cross-sectional dimension. Over millions of test particle there are only hundreds of collisions. (For interpretation of the references to color in this figure legend, the reader is referred to the web version of this article.)

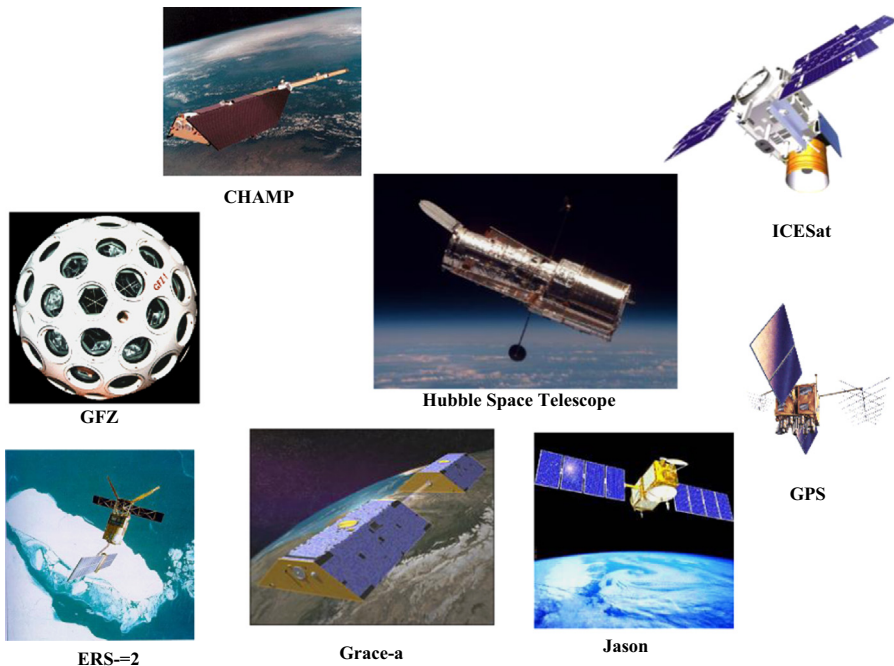


Fig. 18. Sample satellite shapes. While a few satellites have spherical shapes (GFZ), the majority do not. Some satellites exhibit aspect ratios that are near unity, but again, this is not very common. In precise applications, even laser retro reflectors on spheres are observable in OD applications.

4.4. Ballistic coefficient

The previous individual parameters are not known for a majority of the space catalog. Thus, it is common to use a combined parameter which incorporates mass, area, and

coefficient of drag. The ballistic coefficient (BC) is generally recognized as $m/c_D A$, although the reciprocal is used in some places. The ballistic coefficient will vary, sometimes by a large amount. Some research is examining the time-rate of change for this parameter, but not looking at the

variable area, and its effect in the combined factor. It's probably best not to model this parameter, if possible, because it includes several other time-varying parameters that are perhaps better modeled separately.

5. Orbit propagation

At first glance, this may appear to be similar to the next section on orbit determination. However, there is an important difference. In the orbit determination section, the filter can adjust the final state and parameters to match the input observations. Previously, we saw that changing the atmospheric models made a difference, but our comparison was a simulated orbit. The use of independent POEs obviously limits our ability to examine numerous orbits. We also did not use all of the atmospheric models or corrections to models (HASDM, DCA, etc.) as we did not have access to the full model codes, inputs, or implementation in a readily useable form. In this section, we are given a single state and parameters and compare the result to a POE. We then vary the various inputs and show the results. In the absence of the OD processing, we find that the differences are magnified any times.

5.1. Initial state

The uncertainty of the initial state is critical in determining the results of an atmospheric drag perturbed orbit. However, as Vallado [27] shows, even a perfect initial state (< 10 cm radial position) quickly degrades to many

kilometers due to the major perturbation forces. Generic results from this study are shown in the final table.

5.2. Solution method

The integrator type is generally a predictor-corrector, or other high fidelity technique. This factor used to be more

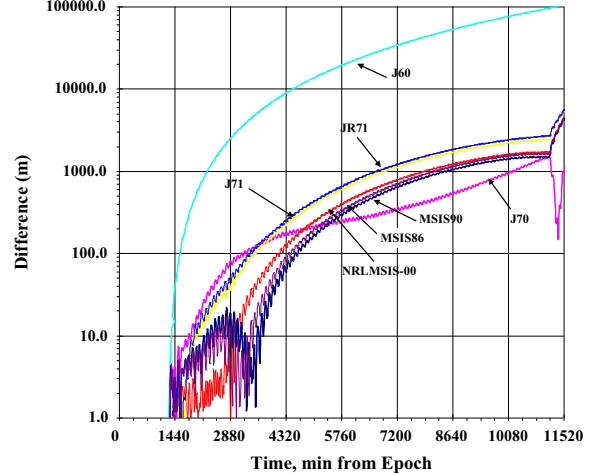


Fig. 19. Sample atmospheric drag sensitivity: Positional differences are shown for ICESat (satellite 27642). The POE comparison was used to evaluate each atmospheric model. Note that each of the atmospheric models used a 3-hourly geomagnetic interpolation, observed solar flux, and a centered 81-day average. The same initial conditions were used for each run.

Table 1

Test setup: Several combinations of treating the input data are analyzed. The labels on the left are simply short-hand to identify each case. Each letter represents a test—last or centered $F_{10.7}$ average, observed or adjusted values to the Earth's radius, and Daily, 3-hourly, 3-hourly interpolated, or spline interpolation for the indices. The final numbers represent the time that the $F_{10.7}$ measurement is assumed to take place—1700 or 2000 UTC.

Name	Fluxfile	Fluxupdate	Drag model	F10OBSTIMEOFDAY	F10MEASUREMENTTYPE	F10AVERAGEMETHOD
Obs3Hr	sw20030101L81Obs.txt	3Hour	Jacchia–Roberts	72,000	Observed	Centered81
ConAll	sw2003ObsConAll.txt	3Hour	Jacchia–Roberts	72,000	Observed	Trailing81
ConAllAvg	sw2003ObsConAllAvg.txt	3Hour	Jacchia–Roberts	72,000	Observed	Trailing81
LOD20	sw2003Obs.txt	Daily	Jacchia–Roberts	72,000	Observed	Trailing81
LAD20	sw2003Adj.txt	Daily	Jacchia–Roberts	72,000	Adjusted	Trailing81
COD20	sw2003ObsC81.txt	Daily	Jacchia–Roberts	72,000	Observed	Centered81
CAD20	sw2003AdjC81.txt	Daily	Jacchia–Roberts	72,000	Adjusted	Centered81
LOT20	sw2003Obs.txt	3Hour	Jacchia–Roberts	72,000	Observed	Trailing81
LAT20	sw2003Adj.txt	3Hour	Jacchia–Roberts	72,000	Adjusted	Trailing81
COT20	sw2003ObsC81.txt	3Hour	Jacchia–Roberts	72,000	Observed	Centered81
CAT20	sw2003AdjC81.txt	3Hour	Jacchia–Roberts	72,000	Adjusted	Centered81
LOI20	sw2003Obs.txt	3HourInterp	Jacchia–Roberts	72,000	Observed	Trailing81
LAI20	sw2003Adj.txt	3HourInterp	Jacchia–Roberts	72,000	Adjusted	Trailing81
COI20	sw2003ObsC81.txt	3HourInterp	Jacchia–Roberts	72,000	Observed	Centered81
CAI20	sw2003AdjC81.txt	3HourInterp	Jacchia–Roberts	72,000	Adjusted	Centered81
LOS20	sw2003Obs.txt	3HourSpline	Jacchia–Roberts	72,000	Observed	Trailing81
LAS20	sw2003Adj.txt	3HourSpline	Jacchia–Roberts	72,000	Adjusted	Trailing81
COS20	sw2003ObsC81.txt	3HourSpline	Jacchia–Roberts	72,000	Observed	Centered81
CAS20	sw2003AdjC81.txt	3HourSpline	Jacchia–Roberts	72,000	Adjusted	Centered81
LOT17	sw2003Obs1700.txt	3Hour	Jacchia–Roberts	61,200	Observed	Trailing81
LAT17	sw2003Adj1700.txt	3Hour	Jacchia–Roberts	61,200	Adjusted	Trailing81
COT17	sw2003ObsC811700.txt	3Hour	Jacchia–Roberts	61,200	Observed	Centered81
CAT17	sw2003AdjC811700.txt	3Hour	Jacchia–Roberts	61,200	Adjusted	Centered81

demanding than today with modern compilers and techniques.

5.3. Propagator

The force model fidelity is important, but most highly accurate programs have the usual full gravity fields, selection of atmospheric models, third body effects, and solar radiation pressure models. The key for precise solutions including atmospheric drag though is the ability to include attitude, albedo, tides (solid, ocean), and thrusting models into the propagation process. This permits a better physically representative model that leaves fewer effects unknown that would increase over time. Vallado [26] presented several plots of different satellites showing the effect of various forces on each orbit. The drag effects dominated the low Earth orbits.

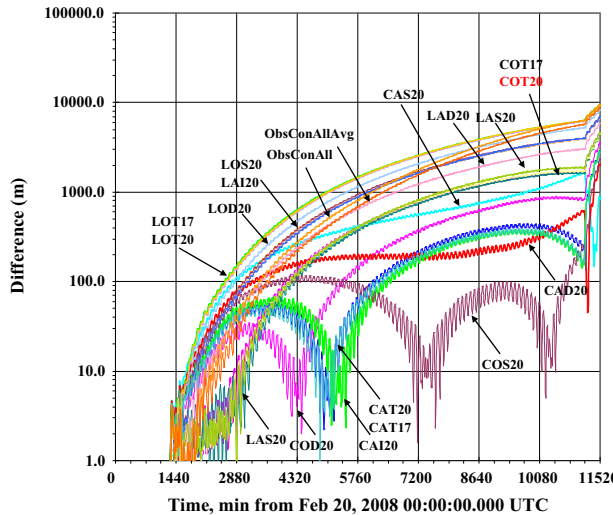


Fig. 20. Sample atmospheric drag sensitivity: Positional differences are shown for ICESat (satellite 27642) using various data approaches with the NRLMSISE-00 model. The POE comparison was used to evaluate each atmospheric model. Note that each of the atmospheric models used a daily interpolation on the geomagnetic indices. The same initial conditions were used for each run, but the axes scales are different.

5.4. Implementation

The selection of one atmospheric model over another evokes lots of discussion. However, it's likely that the selection is not as important as some of the other choices that can be made. In this section, we'll examine the prediction portion in greater detail, varying many of the input parameters (see Table 1 also).

The initial setup for the orbit was as follows. These parameters reflect a reasonable match to Rim and Schutz [19] document but recognize there are no OD's being performed.

70 × 70 EGM-96 gravity
NRLMSISE-00 atm reading a_p values, 3-hourly a_p values
Mass = 950 kg and area = 5.21 m² and c_p = 2.52 (and therefore area/mass ratio = 0.0054842 and BC = 0.0138202)

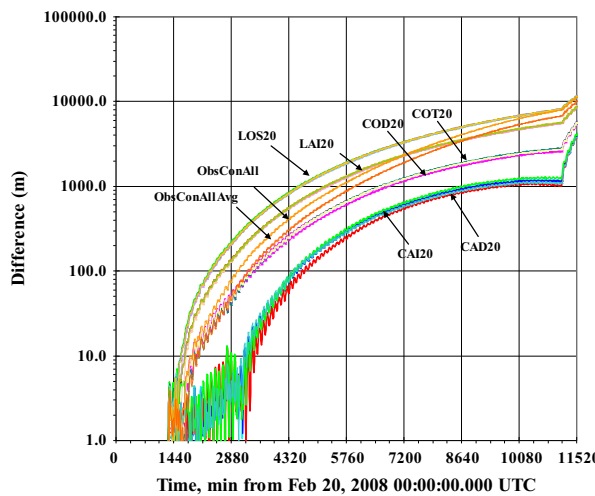
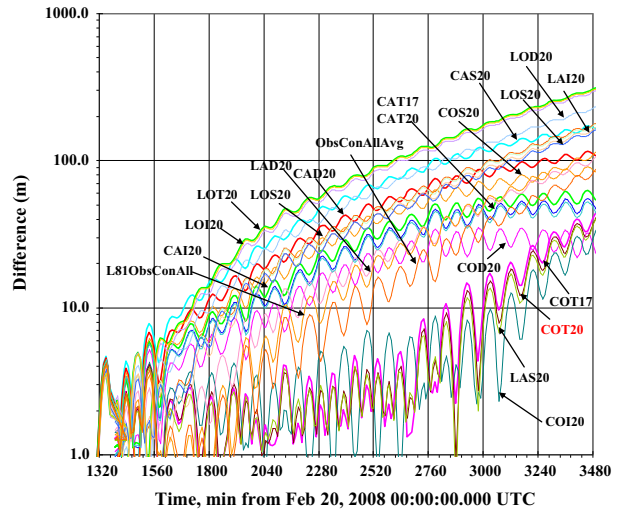
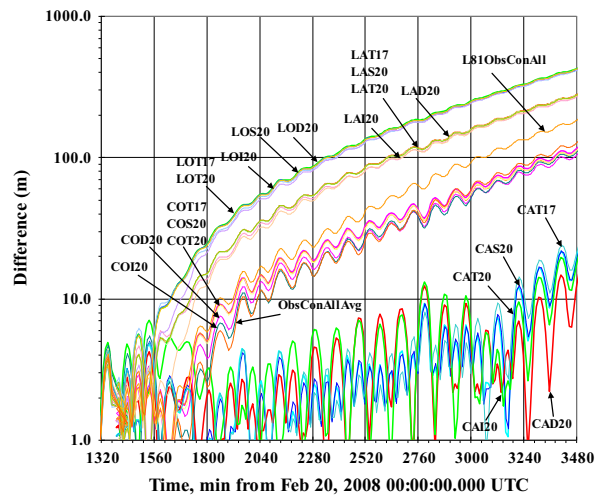


Fig. 21. Sample atmospheric drag sensitivity: Positional differences are shown for ICESat (satellite 27642). The POE comparison was used to evaluate each atmospheric model. Note that each of the atmospheric models used a daily interpolation on the geomagnetic indices. The same initial conditions were used for each run.



Sun and Moon third body
 Solar radiation pressure ($c_{srp}=1.04$) with dual cone boundary mitigation
 Solid and time dependent solid tides and full ocean tides
 RK 7/8 Integrator, relative error of 1×10^{-15} , 1–600 s step sizes
 RIC 5/10/2 m and 0.06/0.04/0.02 m/s

Notice the similarity when comparing to the POE (Fig. 19), to the previous simulated analysis (Fig. 13).

We can also examine the effect of treating the input data differently. Table 1 shows the various test combinations, and the results are shown in Fig. 20.

Using the same configuration as in Fig. 19 we obtain the plots in Fig. 20.

Notice that the short term results are reasonably similar, while the longer term results show a gradual separation of the approaches. After careful study, we could conclude that the centered solar flux generally fared better, and the observed solar flux was also better in most cases. The LAS20 case showed good results in the short term, but quickly degraded in the longer term.

If we use Jacchia–Roberts instead of MSIS inside the filter, we get very different results Fig. 21.

The Jacchia–Roberts results show (much more definitively) that the adjusted solar flux, and centered solar flux averages performed the best, in fact, they differed only by about 1–10 km at the end of a week. The method of interpolation made some minor differences in the short term, but were not a real factor.

The primary difference between the two models was the performance of the adjusted and the observed solar flux in the predictions.

6. Orbit determination

The process of taking the OD from a portion of the POE, and then predicting from that point is a general way to show the interconnectivity of the concepts from the previous sections. The goal here is to examine the propagation performance using the final state from the OD filter run, and then look at different atmospheric models and treatment of the space weather input data. The key is the separate development of the OD for each case. This lets the filter adjust the state (and therefore solve-for parameters) to be optimized for each case, and thus, the propagation is completely consistent and aligned for each test. There are only a few cases presented. Time and availability of POEs were the primary reasons. Although we make conclusions based on such a small sample size, the results should be indicative of general trends and we note this in the final conclusions as well.

The orbit determination and propagation areas are closely linked, but there are some distinctions. Orbit determination encompasses the primary processing of observational data to determine the orbit. As such, the particular form of processing must be very carefully selected to balance the model type, development, and satellite parameters that are available. The assumptions from the atmospheric model development are important, but often overlooked at this step. Some researchers discount the effect of these assumptions in their studies, or

assume that one parameter or model will resolve many of the assumptions. Unfortunately, such considerations must be independently verified and tested to validate the appropriateness of the assertions.

In general, orbit determination imparts some error into the process, but it also can mask many of the parameters discussed earlier in this paper simply by its specific implementation. Often, techniques are applied to mitigate omissions in the force model, model use, model itself, type of processing, etc. These are not wrong, but if they are not coupled with as much physical reality as is known, they are at best incomplete. Thus, while results may achieve a certain level of accuracy in one program, transferring the final state to another program can give dramatically different results. This further stresses the importance of striving to use proper techniques, coding, indices, etc to achieve the best possible results. Documenting the actual practice is perhaps the most important step.

6.1. Observations

The accuracy we obtain from observational data is a function of many variables including the number, type, and quality of the observations in a pass over a sensor, the location of the data within a pass, the total number of tracks, number of sensors, location of the sensors, the processing technique, etc. To obtain the best accuracy, you must trade-off the merits of each of these aspects versus their costs. The Central Limit Theorem implies that more well characterized data is better, and that you will get better results with more data. In other words, the optimal estimate of a state as determined from multiple, independent observations of the same attribute will improve (in a least squares sense) the more observations there are, assuming sufficient quality (variances) of those observations. There are of course limits to how much data can be acquired, but much of the operational space surveillance mission relies on just a very few observations per pass. For limited analytical theories this is sufficient but this is simply not enough when the goal is achieving highly accurate estimates for the orbit. Experiments have confirmed that additional observations can lead to dramatic improvements [18]. In this experiment, AFRL received dense observations directly from a sensor site and processed them with numerical techniques. The resulting vectors were accurate to about 10–15 m as confirmed by laser tests. The comparable AFSPC vector produced with a handful of observations per pass and somewhat limited force models produced a vector only accurate to about 400 m, again confirmed by laser tests.

The inherent noise in the observations makes it all that more difficult to properly use the time changing space weather parameters. Thus—if one treatment of the space weather parameters works better in an OD, is it because the process was correct, or it accounted for an inconsistency in the observational data? We'll see this shortly.

6.2. Solution method

Batch least squares (BLS) and Kalman filter methods are most common for orbit determination. BLS methods have

an inherent difficulty when processing LEO satellite data—the fit span is generally a few days. Over this time, the satellite may make 40–60 or more revolutions. Averaging the observations reduces the amount of information which may be extracted for solution. Some success has been accomplished with “track weighting” and segmented parameters in which individual tracks or parameters are processed or accounted for in the orbit determination. However, this is a simplistic short cut to accurately processing each measurement. Kalman filters avoid the ambiguities and additional required logic to account for long fit spans and permits a dynamic evaluation of all parameters. Determining the proper dynamic modeling of sensor and satellite parameters can be a challenge. We tend to lean with Kalman filter approaches because it is evident that sensor and satellite parameters will vary over time.

Maneuvers present yet another difficulty in orbit determination. BLS methods may be configured to process

position and velocity vectors (km and km/s) from the POE are (osculating orbital elements are included for each time) are

From the filter OD, the residual ratio and smoother position uncertainty are shown in Fig. 22.

A unique report in ODTK is the filter-smoother consistency test. The report is found using the filter and smoother runs. Essentially, the report is an instantiation of the McReynolds filter-smoother consistency test. It states that the difference of the filter and smoother runs is a zero mean Gaussian vector with a covariance given by the difference of the two covariances. The differences let you examine the transponder, station biases, ballistic coefficient, atmospheric density, etc. to determine if the filter modeling is proper. The position consistency check is shown in Fig. 23. Note that the results should all fall within the ± 3 limit. If the modeling is off in any parameter, the test will exceed the ± 3 limit.

POE 19 Feb 2003 20:59:47.000 UTCG 814.732027000 – 6735.434964000 1620.790872000 – 0.8173538675 – 1.8748560790 -7.3333578195
POE 20 Feb 2003 20:59:47.000 UTCG 791.990709000 – 4288.658540000 5435.575745000 – 0.0759493638 – 5.9813522276 – 4.6964130956
a e incl raan argp nu m
POE 19 Feb 2003 20:59:47.000 UTCG 6979.966219 0.001583 93.992 200.242 100.611 65.935 65.770 0.013820 1.04
POE 20 Feb 2003 20:59:47.000 UTCG 6969.395729 0.001219 93.995 200.751 41.976 86.606 86.467 0.013820 0.01403 1.073359

through a maneuver, but the usual technique requires a restart. If the maneuver is long, or even a continuous thrusting application, BLS techniques will fail. Kalman filters can actually process through maneuvers and because the maneuver can be input to the process, the recovery time after a maneuver is significantly reduced, usually within a revolution of the maneuver.

6.3. Implementation

We expand the earlier results and perform OD to demonstrate the previous discussions. Consider a POE from 2003 for ICESat. The reference ephemeris (POE) is usually accurate to about 10–20 cm radial position throughout the interval so we will consider that to be truth for our purposes. We can then try several orbit determination options (as with the previous sections) and observe the effects. Using a force model setup of

70 × 70 EGM-96 gravity
Solid and time dependent solid tides and full ocean tides
NRLMSISE-00 atm using observed $F_{10.7}$ values, and 3-hourly a_p values
Mass=950 kg and area=5.21 m ² and $c_D=2.52$ (and therefore area/mass ratio=0.0054842 and BC=0.0138202)
Sun and Moon third body
Solar radiation pressure ($c_{srp}=1.04$) with dual cone boundary mitigation
RK 7/8 Integrator, relative error of 1×10^{-15} , 1–600 s step sizes
RIC 5/10/2 m and 0.06/0.04/0.02 m/s

we run the filter for 1 day using the POE ephemeris states as observations. The Earth Fixed (ITRF) initial and final

The resulting state from the filter is shown below. The original values from the POE are given in red. Notice the proximity of the values. Although we could take the state directly from the POE and use the published force models in the development of the POE, it is more accurate to insert an additional OD into the process to ensure the force models line up exactly. We discussed this previously, and we repeat it here because it's important. The inclusion in the development of independent POE's of 1 cycle per revolution parameters, process noise, solve for parameters, polynomial approximations, etc, make it virtually impossible to precisely line-up the force models exactly between different programs.² The results are significantly more realistic if an additional OD is conducted. However, we compare to the original POE for maximum accuracy. It would be disingenuous to compare to an ephemeris created by our OD run, and would negate any benefit of the comparison to an independent reference source.

Fig. 24 shows both the performance after the filter (the first day), and during the prediction until the time of the first maneuver (about Feb 27, 2008). Several options are run for comparison to the earlier figures. Unlike the previous sections though, a separate OD is performed for each case. All cases were run with the time of the solar flux measurements set to 20:00 h UTC.

While NRLMSISE-00 suggests that no interpolation is needed, the best performance in Fig. 24 comes from the splined results. The double-hump shape of the CAS run in

² The level of coordination is remarkable to line-up propagators [26] ut propagation is just a small subset of the available operations in OD.

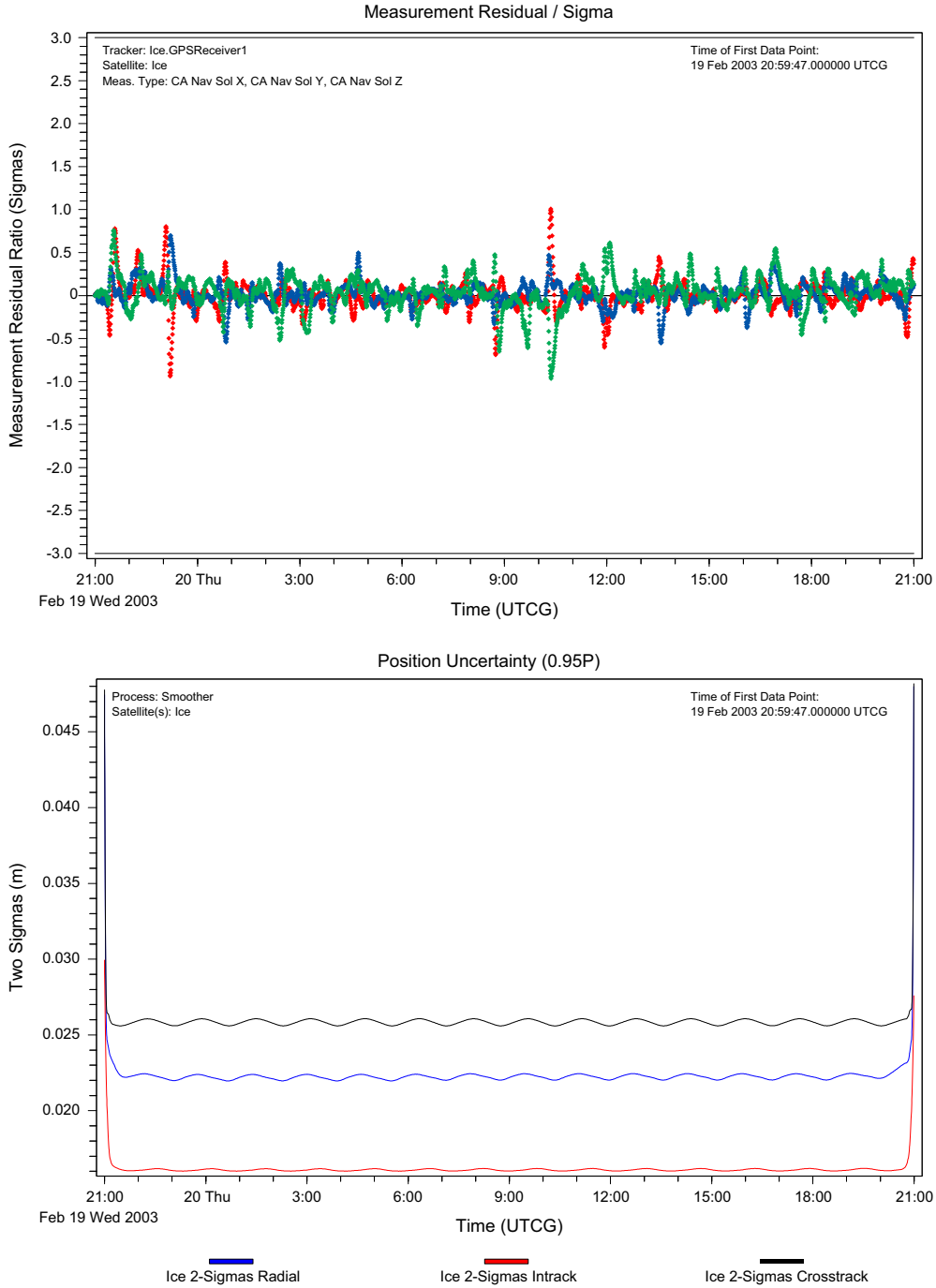


Fig. 22. Filter results for ICESat processing: The residual ratios (left, residuals divided by the sigma values) and the position uncertainty (right) are shown. Note that the filter is estimating the orbit to about 15 cm.

[Fig. 24](#) suggests it may be an artifact of the processing and not an actual repeatable result for many orbits. Thus, we decided to run a similar experiment for ICESat, but at a different time. [Fig. 25](#) shows the results. Note that although the interval coincided with an unusually large spike in the solar flux, the results are “roughly” similar to [Fig. 24](#), but the scale is about twice as large in [Fig. 25](#) as in [Fig. 24](#).

It would take many more trials, to find a definitive range of values we could expect from different atmospheric models and treatment of the input data, but these limited cases indicate the simulated and actual results are both within the 1–10 km range. Thus, the simulated results are probably correct to at least the same order of magnitude. However, the actual (OD) results are a “little” less than some of the differences we saw in the propagation section. It follows that

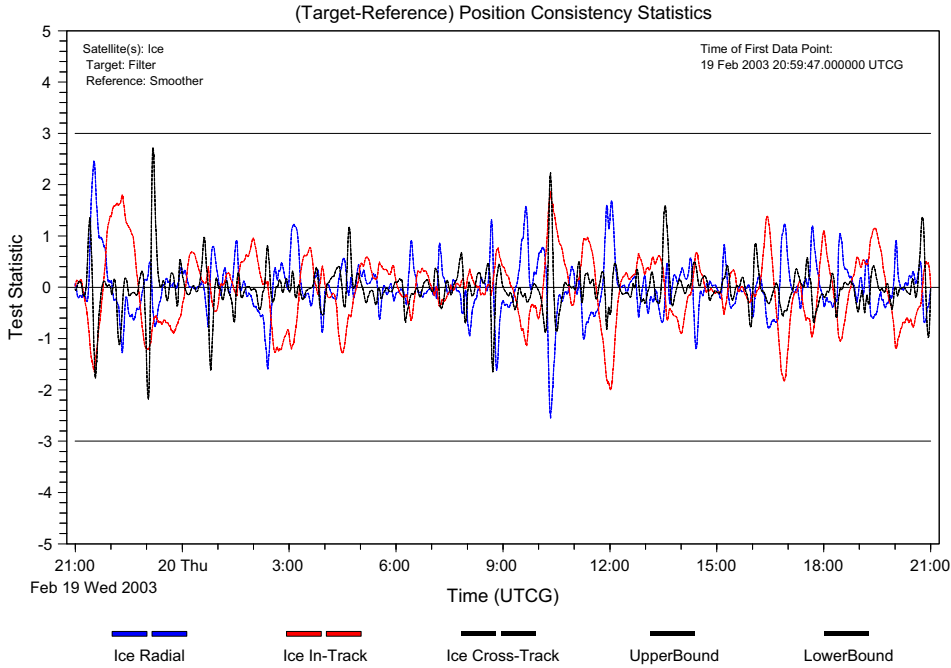


Fig. 23. Filter smoother results for ICESat processing: The position consistency test is shown for the day that the filter was run. Note that all the points are well within the limit of 3. This gives us added confidence that the modeling is sufficient.

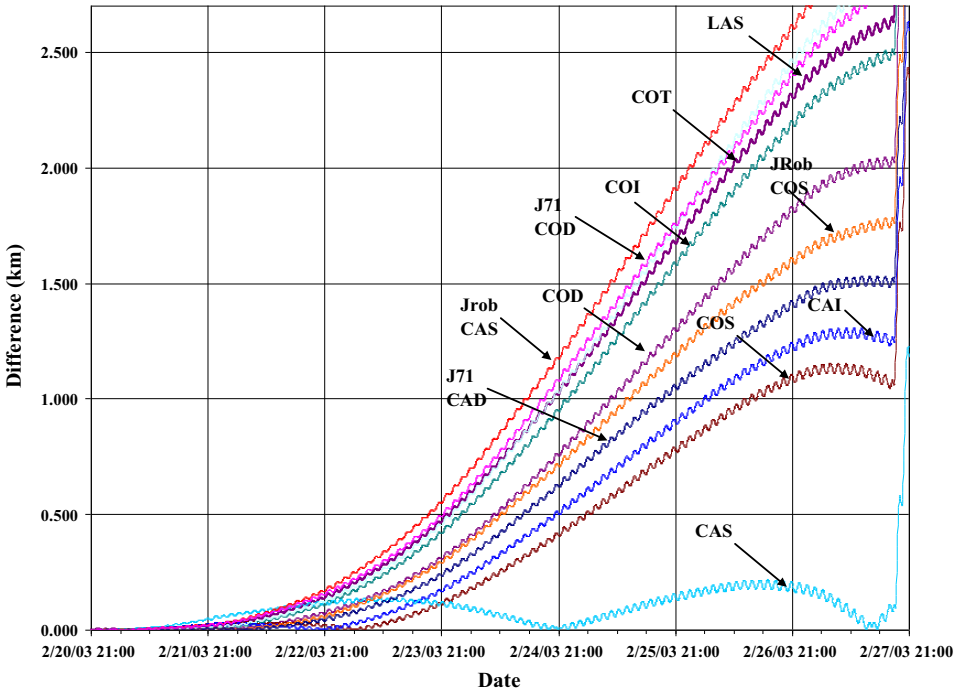


Fig. 24. Prediction results for ICESat processing in Feb 2003: The position uncertainty is shown for a one day filter-smoother run using the NRLMSISE-00 atmospheric model. The filter portion is not shown. Some alternate atmospheric models are used as indicated. The noise at the end of the span is a small maneuver in the ephemeris. The options specify the centered or last 81 day averages, observed or adjusted solar flux, and the treatment of solar flux, daily, 3-hourly, 3-hourly interpolated, or 3-hourly splined. Note that the NRLMSISE-00 model is generally better than comparable approaches with other models.

the effect should not be as great because the orbit determination program is simply using the atmospheric model to estimate the density, and the OD will arrive at a slightly

different solution using a different atmospheric model. That one filter state produces more accurate results than another is simply a consequence of the individual solution.

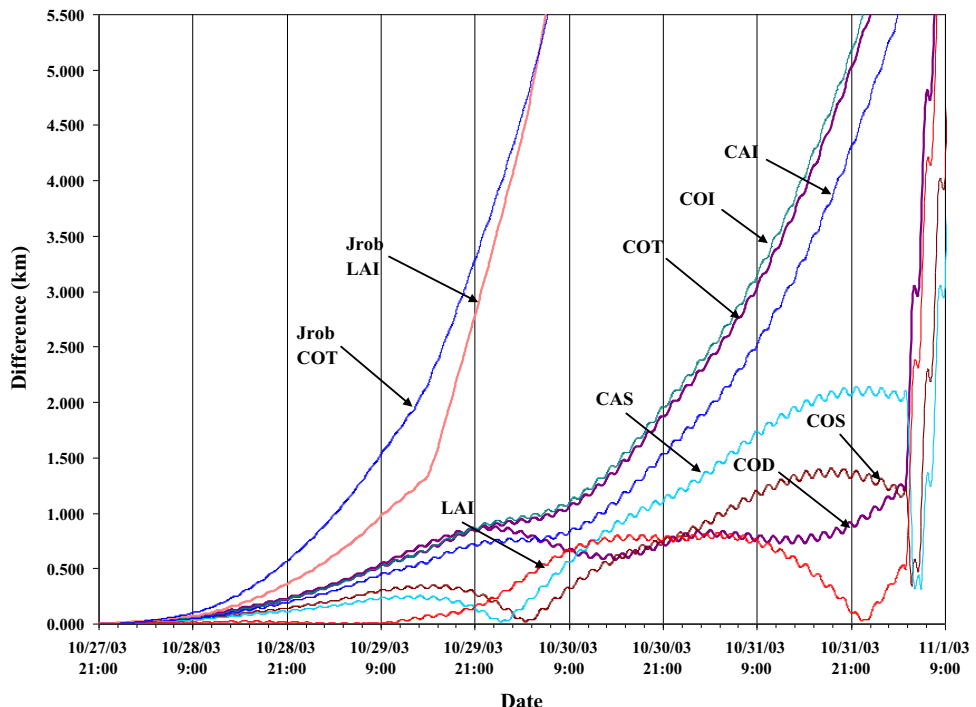


Fig. 25. Prediction results for ICESat processing in Nov 2003: The position uncertainty is shown for a one day filter-smoother run using the NRLMSISE-00 atmospheric model, and some others. The one day filter interval is not shown. Several approaches for using the input data are shown. The options specify the centered or last 81 day averages, observed or adjusted solar flux, and the treatment of solar flux, daily, 3-hourly, 3-hourly interpolated, or 3-hourly splined. Although the curves are different from Fig. 24, the NRLMSISE-00 model still seems to perform better than JRob or J71.

6.4. Implementation using observations

Finally, we investigated a different satellite to determine if the results would be consistent. The CHAMP satellite is at about 400 km altitude, and thus provided a different look for the analysis. An independent POE was not available for this satellite, so we used GPS measurements and processed a large set of data to produce a reference orbit (RO). Based on the filter-smoother consistency test, we are confident this orbit is accurate to about 20–30 cm throughout the 2-week interval which is sufficient for our purposes, but we'll retain the “reference orbit” label to distinguish it from an independent POE. The initial orbital parameters were set as follows: (web references included the following)

http://www-app2.gfz-potsdam.de/pb1/op/champ/systems/index_SYSTEMS.html
<http://www.gfz-potsdam.de/pb1/CHAMP/satellite.htm>
 champ 91 deg incl 347 km, NORAD SSC# 26405

70 × 70 EGM-96 gravity
 Solid and time dependent solid tides and full ocean tides
 NRLMSISE-00 atm reading a_p values, 3-hourly a_p values
 Mass=510 kg and area=0.72036 m² and $c_D=2.2$, (and therefore area/mass ratio=0.0014125, and BC=0.0031074)
 Sun and Moon third body, use variational equations
 Solar radiation pressure ($c_{srp}=1.0$) with dual cone boundary mitigation
 RK 7/8 Integrator, relative error of 1×10^{-15} , 1–600 s step sizes
 Be sure GPS constellation COM, uncertainty 1-2-1m defaults
 Be sure GPS receiver all meas stats

Be sure CHAMP all meas types, RIC uncertainty 5–10–5 cm,
 0.001 m/s
 RIC 1.0/2.0/1.0 m and 0.01/0.01/0.01 m/s

We run the filter for 1 day as we did with ICESat. The Earth Fixed (ITRF) initial and final position Fig. 26

Notice the rapid departure from the reference orbit. Also notice that the reference orbit was generated with the NRLMSISE-00 model, COT, but that combination for the shorter filter and prediction performed the worst of any of the options. This effect is still under investigation.

6.5. Additional discussion

It appears that whether or not we solve the area to mass ratio, and/or use c_D and density, the OD process absorbs much of the errors and arrives at a solution with the proper “energy”, based on those initial conditions. Stipulating certain density values, BC, and therefore c_D , a , and m , restricts solutions to the precise implementation that developed the original parameters. Furthermore, this limits interoperability due to the rigorous and extremely intricate requirements needed to align all the nuances and implementations of OD programs. Another set of input conditions will arrive at a different, but equally valid, and potentially better solution to predict into the future.

Thus, we again state that every attempt should be made to include as much physical realism as possible in the

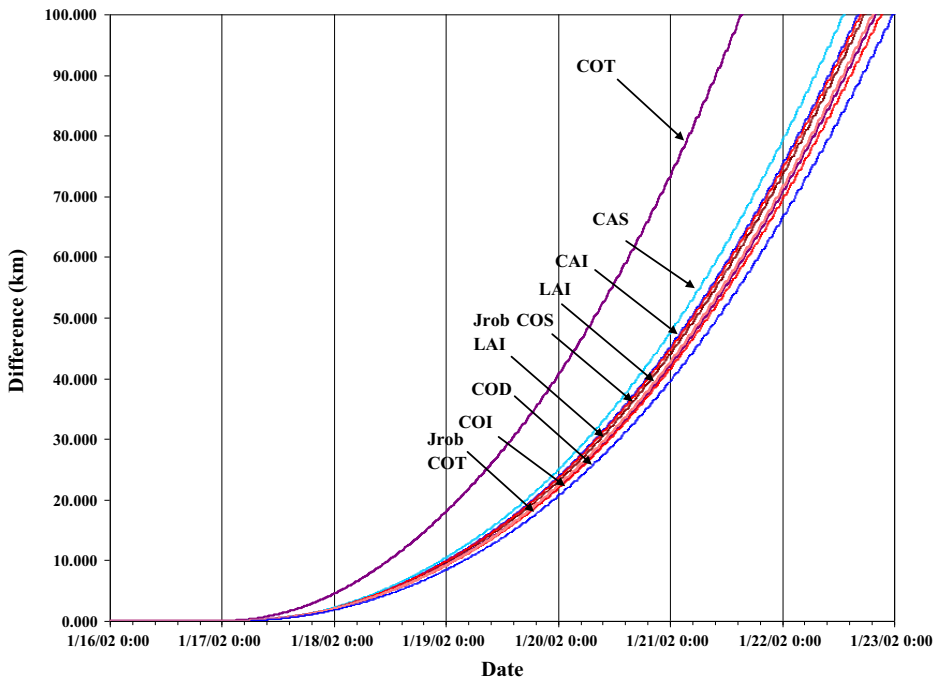


Fig. 26. Prediction results for CHAMP Processing in Jan 2002: The position uncertainty is shown for a filter-smoother run using the NRLMSIS-00 atmospheric model and several options. The options specify the centered or last 81 day averages, observed or adjusted solar flux, and the treatment of solar flux, daily, 3-hourly, 3-hourly interpolated, or 3-hourly splined.

setup and use of an OD system. Pre-determined density, c_D , BC, etc values are only a guide and cannot be reliably used for detailed studies unless extensive development work is done to establish the precise line-up of individual OD system approaches to include all the aspects addressed in this paper.

7. Summary and conclusions

The proceeding discussion has provided numerous options for consideration in using atmospheric drag for propagation and OD, and in understanding why differences exist between various implementations. Unfortunately, there is no single recipe for choosing among the numerous alternatives of models and processes discussed in this paper. Experience and expertise guide the most appropriate choices for each investigator. The goal is to understand why there are differences and with the results reported in this paper, to seek a balanced approach to anticipate what the differences might be, and to try and mitigate them. In some cases, our conclusions were developed from small sample sizes consistent with the availability of POEs. Thus, the results are intended to be general in nature, and not specific to a certain satellite, or class of satellites. The overall goal was to quantify the expected behavior of various factors that should be considered when using atmospheric drag. Several important conclusions follow.

- No single atmospheric model is best for all applications. Bruinsma et al. [2] states this as follows: “JB2008 is the most accurate model below 300 km, JB2008 and DTM

2009 perform best in the 300–500 km altitude range, whereas above 500 km NRLMSISE-00 and DTM2009 are most accurate. The precision of JB2008 decreases with altitude, which is due to its modeling of variations in local solar time and seasons in particular of the exospheric temperature rather than modeling these variations for the individual constituents.” Another example is the use of an atmospheric model to substantiate a lifetime provision from international standards. A new model that performs well during the interval of data in which it was developed may not perform well 3–4 solar cycles later when the solar cycles are only $\frac{1}{2}$ to $\frac{1}{4}$ the cycles in the historical record.

- The propagation differences between atmospheric density models are about the same magnitude as treating the input data differently. A particular set of input conditions (satellite parameters, atmospheric models, use of indices, force models and solution method) will achieve a solution. A different initial set of input conditions may arrive at a different equally valid, but potentially better solution to predict into the future.
- Attempting to use one or two fixed parameters may result in improved results, but unless the underlying assumptions and conventions are precisely known and based on an understanding of the physics (which they are often not), you simply shift the problem from one variable to another. Depending on your solution technique, this may make certain problems unobservable and give you a false outcome.

We summarize the major choices and their approximate effects in Table 2 below.

Table 2

Atmospheric drag summary and effects: Each of the various topics discussed is identified with a brief summary of the topic, and numerical results if available. Unless each of these characteristics are well known and appropriate, results are suspect. Note that the effects are cumulative.

Topic	Summary of topic	Effect
Atmospheric model development		
Indices	Which indices available when developed? How were they used? Span of time indices available	
Data used in generation	Satellites were limited in atmospheric model development	
Orbital class	Atmospheric model is only good for certain orbital classes	
Fidelity	Many studies, no conclusive “winner”	10–15% or more inaccuracy
Atmospheric model use		
Which model	Jacchia, MSIS, DTM, JB08, etc.	100 to 50,000 m in 4 days
Implementation	Code implements technical approach exactly?	??
Accuracy	Inherent inaccuracy of the model	10–15%
Data indices availability	Publicly available? Time span available	??
Data correction	Observed vs adjusted	6,000 m in 4 days
Daily vs hourly values	Frequency of updates to indices	3,000 m in 4 days
Interpolation	Interpolate or not	10–5,000 m in 4 days
	Which parameters to interpolate, or all?	3,000 in 4 days
	Method of interpolation	10–20 m
Which index to use	Use a_p or K_p preferentially?	??
Time lags	6.7 h, other	??
Time of observation	1700 vs 2000 UTC for $F_{10.7}$	1,000 m in 4 days
Averages	Centered or trailing?	10,000 m in 4
Prediction	Source, Schatten, ESA, Oltrogge, Other?	120–150 SFU (long)
	Variability over time	Varies
	Short term accuracy	1–5 SFU (short)
Winds		??
<i>All previous categories</i>		
Satellite parameters		
Mass	Accuracy	5–10%
Area	Time varying?	??
c_D	Aerodynamics, gas dynamics, continuum flow	??
Model detail	Sphere, plate models, detailed CAD	??
Attitude known	Consider a 10 m long 3 m diameter cylinder end vs side	424% difference
Materials	Interaction to atmosphere—DSMC method?	??
Maneuvers	Known or unknown	Can be very large
	Magnitude, direction	100's of km
Orbit propagation		
Input state accuracy	Example 1 m initial error in the position	5,000–10,000 m in 7 days (extrapolated)
Integrator type		Small
Force model fidelity	Drag force is 10–100 km or more effect in 4 days	Varies
<i>All previous categories</i>		
Orbit determination		
Obs quality	Not tested	400 m at epoch
Obs quantity	Phillips Lab (1995) report	??
Solution method BLS	Not tested	
Solution EKF		
Force models	Using a different atmospheric model	500–10,000+ m in 7 days
<i>All previous categories</i>		

References

- [1] F. Barlier, et al., A thermospheric model based on satellite drag data, *Ann. Geophys.* 34 (1) (1978) 9–24.
- [2] L. Sean, Bruinsma, et al., Evaluation of the DTM-2009 thermosphere model for benchmarking purposes, *J. Space Weather Space Clim.* 2 (2012) A04.
- [3] Doornbos, Eelco, N. 2011. Thermospheric Density and Wind Determination from Satellite Dynamics. Ph.D. Dissertation. Technical University Delft.
- [4] Gaposchkin, E. M. 1994. Calculation of Satellite Drag Coefficients. Technical Report 998. MIT Lincoln Laboratory, MA. [10].
- [5] E.M. Gaposchkin, A.J. Coster, Analysis of satellite drag, *MIT/LL J. Fall* 1 (2) (1988) 1988.
- [6] P. Graziano Benjamin, 2007. Computational Modeling of Aerodynamic Disturbances on Spacecraft within a Concurrent Engineering Framework. Ph.D. Dissertation. UK: Cranfield University, School of Engineering.
- [7] A.E. Hedin, MSIS-86 thermospheric model, *J. Geophys. Res.* 92 (1987) 4649–4662.
- [8] L.G. Jacchia, 1965. Static Diffusion Models of the Upper Atmosphere with Empirical Temperature Profiles. *Smithsonian Contributions to Astrophysics*. 8. 215–257.
- [9] L.G. Jacchia, 1970. New Static Models for the Thermosphere and Exosphere with Empirical Temperature Profiles. *SAO Special Report No. 313*. Cambridge, MA: Smithsonian Institution Astrophysical Observatory.
- [10] L.G. Jacchia, 1971. Revised Static Models for the Thermosphere and Exosphere with Empirical Temperature Profiles. *SAO Special Report No. 314*.

- No. 332. Cambridge, MA: Smithsonian Institution Astrophysical Observatory.
- [11] H. Klinkrad, Fritzsche, B. 1998. Orbit and Attitude Perturbations due to Aerodynamics and Radiation Pressure, ESA Workshop on Space Weather, ESTEC, Noordwijk, Netherlands.
- [12] G. Koppenwallner, B. Fritzsche, 2006. Multidisciplinary Analysis Tools for Orbit and Reentry, Hyperschall Technologie Goettingen, Kallenburg-Lindau, Germany, presented at the Third International Workshop on Astrodynamics Tools and Techniques, ESTEC, Noordwijk, Netherlands.
- [13] J. Kork, Satellite Lifetimes, Chapter V. Design Guide to Orbital Flight, McGraw-Hill, New York, 1962.
- [14] A. Marcos Frank, et al. 1993. Satellite drag models: current status and prospects, in: Paper AAS-93-621 presented at the AAS/AIAA Astrodynamics Specialist Conference. Victoria BC, Canada.
- [15] F.A. Marcos, W.J. Burke, S.T. Lai, 2007. Thermospheric Space Weather Modeling. Air Force Research Laboratory Report, ADA471447.
- [16] Oltrogge, Daniel L., Chia-Chun Chao. 2007 Standardized approaches for estimating orbit lifetime after end-of-life, in: Paper AAS 07-261 presented at the AAS/AIAA Space Flight Mechanics Conference. Mackinac, MI.
- [17] J.M. Picone, A.E. Hedin, D.P. Drob, NRLMSISE-00 empirical model of the atmosphere: statistical comparisons and scientific issues, *J Geophys Res* 107 (A12) (2002) 1468.
- [18] Phillips Laboratory. 1995. 1995 Success Stories. Kirtland Air Force Base, NM: Phillips Laboratory History Office.
- [19] H.J. Rim, B.E. Schutz, 2002. Geoscience Laser Altimeter System (GLAS), Algorithm Theoretical Basis Document, Ver 2.2 Precision Orbit Determination (POD). Center for Space Research, The University of Texas at Austin.
- [20] H. Kenneth Schatten, S. Sofia, Forecast of an exponentially large even-numbered solar cycle, *Geophys. Res. Lett.* 14 (1987) 632–635.
- [21] L.H. Sentman, Comparison of the exact and approximate methods for predicting free-molecular aerodynamic coefficients, *Am. Rocket Soc. J.* 31 (1961) 1576–1579.
- [22] Tanygin, Sergei, James R. Wright. 2004. Removal of arbitrary discontinuities in atmospheric density modeling, in: Paper AAS 04-176 presented at the AAS/AIAA Space Flight Mechanics Conference. Maui, HI.
- [23] G. Thuillier, S. Bruinsma, The MgII Index for upper atmosphere modeling, *Ann. Geophys. Eur. Geophys. Soc.* v19 (2001) 219–228.
- [24] A. Vallado David, T.S. Kelso. 2005. Using EOP and space weather data for satellite operations, in: Paper AAS 05-406. AIAA/AAS Astrodynamics Specialist Conference and Exhibit. Lake Tahoe, CA.
- [25] A. Vallado David, T. S. Kelso, 2013. Earth Orientation Parameters and Space Weather data for Flight Operations. Paper AAS 13-373 presented at the AIAA/AAS Space Flight Mechanics Meeting. Kauai, HI.
- [26] A. Vallado David, 2005. An analysis of state vector propagation using differing flight dynamics programs, in: Paper AAS 05-199 presented at the AAS/AIAA Space Flight Mechanics Conference. Copper Mountain, CO.
- [27] A. David Vallado, Fundamentals of Astrodynamics and Applications, fourth ed, Microcosm, Hawthorne, CA, 2013.